Project 1

THE INFLUENCE OF PBF ON P53 AND RAD6 IN THYROID CANCER

Project 2

OESTROGEN METABOLISM IN COLORECTAL CANCER

BY

LORNA CATHERINE GILLIGAN

A thesis submitted to the University of Birmingham for the degree of MRES BIOMEDICAL RESEARCH- (MOLECULAR AND CELLULAR MEDICINE)

College of Medical and Dental Sciences

University of Birmingham

August 2012

ACKNOWLEDGEMENT

I would like to show my gratitude to both of my supervisors, Prof. Chris McCabe and Dr Paul Foster, for all of their help in guiding me through these projects. I thank you for being both encouraging as well as challenging. I would also like to offer a special thank you to Anne-Marie Hewitt who is a wonderful teacher, advisor and technician. In addition I would like to thank all of my colleagues on IBR floor 2 for their support.

CONTENTS

Project 1: The Influence of PBF on p53 and Rad6 in Thyroid Cancer

List of Illustrations

List of Tables

Project 1

THE INFLUENCE OF PBF ON P53 AND RAD6 IN THYROID CANCER

This project is submitted in partial fulfilment of the requirements for the award of the MRes.

ABSTRACT

PTTG binding factor (PBF) has been implicated in many cancers, including thyroid. One of the main treatments for thyroid cancer is ablation using I^{131}. Previous research has shown PBF can inhibit I^{131} uptake into the thyroid, which may account for some cancer recurrence. Unpublished data has shown PBF can bind to and inactivate p53, disrupt DNA repair, induce genetic instability and cause a two-fold rise in the E2 ligase DNA repair protein Rad6. Rad6 is known to form a complex with p53 and aids regulation of p53 cellular levels. The aim of this project was to determine if PBF binds to and promotes Rad6 to impair DNA repair using siRNA, transfection, Western blotting and Co-Immunoprecipitation techniques. Results found that knock down of Rad6 lowered p53 levels and overexpressed Rad6 resulted in an abnormal Rad6-p53 co-localisation. Also, as PBF can induce Rad6, Rad6 can also induce PBF. In conclusion increased Rad6 expression resulted in an abnormal, perhaps oncogenic, interaction with p53, but it is still unknown if PBF binds to Rad6 inhibiting DNA repair capacity.

1.0 INTRODUCTION

1.1 The Thyroid

The thyroid is one of the largest endocrine glands, weighing about 20g. Situated in the neck, this butterfly shaped gland's main function is to regulate metabolic rate. It does this through the active uptake of iodine via the sodium-iodide symporter (NIS), to produce the hormones L-thyroxine (T4) and triiodothyronine (T3) and secrete them directly into the bloodstream. On binding to receptors these hormones, particularly T3, alter gene transcription and so production of various proteins involved in cellular metabolism and growth. The thyroid gland is also involved in maintaining blood calcium levels through the release of calcitonin (1, 2). Figure 1 demonstrates the position and anatomy of the thyroid gland (3, 4).

Figure 1.

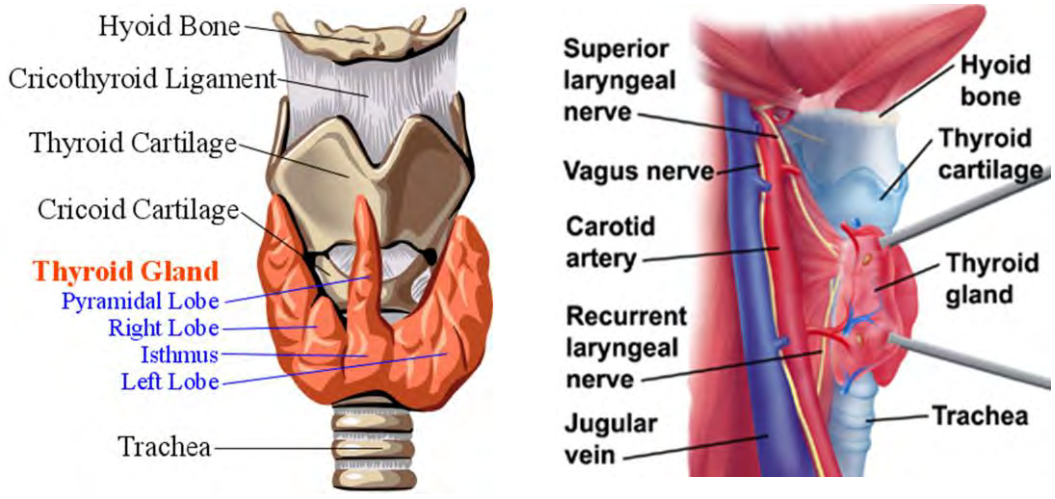

Figure 1. Picture demonstrating the anatomy of the thyroid gland and its surrounding structures (3, 4).

The thyroid gland's production, storage and secretion of thyroid hormones are controlled by a negative feedback loop as shown in Figure 2 (5).

Figure 2.

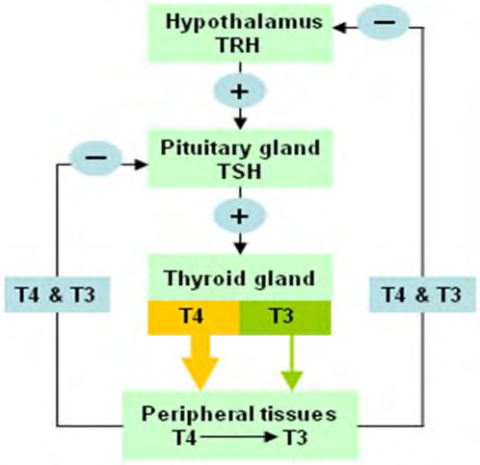

Figure 2. Flow diagram of the hypothalamus-pituitary-thyroid axis. This negative feedback loop maintains appropriate levels of peripheral T3 and T4. Thyroid releasing hormone (TRH), thyroid stimulating hormone (TSH) (5).

1.2 Thyroid Cancer

Thyroid cancer accounts for 1% of all cancers in England with 1,800 new cases occurring annually in England and Wales. It is three times more common in women than in men and usually diagnosed in people aged between 30 and 50. There are four main types of thyroid cancer with papillary carcinoma being the most common followed by follicular thyroid cancer. Medullary thyroid cancer and anaplastic thyroid cancer are both rarer (1). General symptoms include the appearance of a lump on the gland, voice hoarseness, difficulty swallowing or breathing and pain in the neck or throat. A significant risk factor for thyroid cancer is ionising radiation exposure, such as from radiotherapy (1). However, the most memorable are the effects from the atomic bombs in Nagasaki and Hiroshima in Japan in 1945 and the accident at Chernobyl nuclear reactor in the Ukraine in 1986. Here cases of thyroid cancer remain high, particularly amongst those who were children or adolescents at the time of the incidents. In addition there are likely to be similar effects from the recent nuclear accident in Fukushima, Japan in 2011 (6, 7). A higher incidence of thyroid cancer is

associated with hereditary familial adenomatous polyposis and for medullary thyroid cancer multiple endocrine neoplasia (MEN 2A, MEN 2B) and familial medullary thyroid carcinoma (FMTC) (8).

Current treatment for thyroid cancer is surgical removal of the thyroid and/ or radioactive iodine treatment (I^{131}). Surgery does risk damaging surrounding structures in the neck as seen in Figure 1 above. For example, recurrent laryngeal nerve damage can lead to vocal cord paralysis and if the parathyroid glands are removed, then life-threatening hypocalcaemia can occur. As the thyroid gland actively uptakes the majority of iodine through NIS to produce thyroid hormones, I^{131} as a treatment can selectively target and ablate the thyroid gland. Removal of the thyroid through surgery and I^{131} results in patients requiring thyroid hormone replacement for the remainder of their lives. However, thyroid replacement, through negative feedback shown in Figure 2, does lower TSH levels, which has been found to reduce the risk of recurrent disease (8). Many factors affect prognosis, including stage of disease at diagnosis and type of cancer. Overall current treatment provides excellent survival; in particular for papillary and follicular types, with 10 year survival of 90% and 80% respectively. In comparison anaplastic thyroid cancer has a very poor prognosis even if diagnosed in the early stages; as few as 20% will survive 5 years or more. Even for those thyroid cancers with good prognosis, recurrence is a considerable problem, some studies have quoted as high as up to 30% and recurrence is harder to treat (8, 9, 10). Understanding why some tumours are more likely to recur than others and targeted treatment focusing on reducing recurrence would be of great benefit and reduce mortality from thyroid cancer.

1.3 PTTG and PBF

Pituitary tumor-transforming gene (PTTG), isolated in 1997, is a multifunctional protein overexpressed in many cancers, including pituitary and thyroid. Also known as the human

securin (11), PTTG can induce cellular transformation and is associated with more aggressive tumours (12). PTTG binding factor (PBF) was discovered via its interaction with PTTG and is thought to promote the nuclear localisation of PTTG. PBF is a ubiquitously expressed small protein (22kDa) located on chromosome 21q22.3 and like PTTG has transforming ability, is overexpressed in numerous cancers including thyroid and is associated with early disease recurrence. PBF is highly conserved between species suggesting a distinct function and evolutionary importance; however, its primary function is still unknown. PBF can independently induce and advance tumourigenesis (11, 12, 13) and subcutaneous expression leads to tumours in athymic nude mice (14). Also PBF has a role in regulating NIS in thyroid cells (15, 16). PBF overexpressed *in vivo*, specifically in the thyroid, attenuated NIS function and led to hyperplastic growth and macrofollicular thyroid lesions (17). A reduction in NIS function would diminish iodine uptake into the thyroid, including I^{131} used in the treatment of thyroid cancer. Studies such as those mentioned above suggest PBF and PTTG are potential therapeutic targets. If manipulated they could increase I^{131} uptake, improving treatment of thyroid cancer and consequently decreasing the percentage of recurrent disease and mortality.

1.4 p53

p53 is a well characterised protein known as the guardian of the genome. Its role is to halt the cell cycle and initiate DNA repair, senescence or apoptosis (18). Cellular levels are tightly controlled by multiple pathways and under normal circumstances are kept low via the ubiquitin proteasome degradation pathway; p53 is polyubiquitinated by mdm2 and Rad6 to signal it for proteasome breakdown. Figure 3 shows that during stress, such as DNA damage, p53 stabilises and accumulates. Less p53 is polyubiquitinated during stress and Rad6, uncoupled from the p53-mdm2-Rad6 ternary complex, is able to bind to the promoter and coding regions of the p53 gene, consequently increasing levels of histone methylation and p53 transcription (18).

Figure 3.

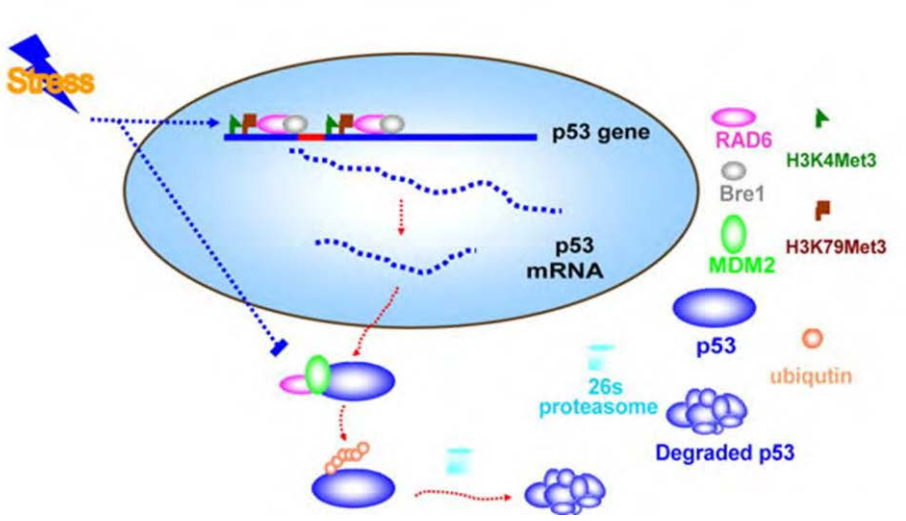

Figure 3. Diagram of the pathways in which Rad6 regulates p53. During cell stress Rad6 can bind to the promoter coding regions of the p53 gene, increasing histone methylation, leading to p53 transcription. Rad6 can also form a complex with MDM2 causing polyubiquitination of p53, signalling it for degradation (18).

p53 is a tumour suppressor and mutations occur in 50% of all cancers (19). Also, expression of its critical regulators, such as mdm2, mdm and Arf are frequently disrupted in cancer. PBF functions as a proto-oncogene and recent (unpublished) data have found an interaction with p53. PBF can bind to and functionally inactivate p53, disrupt p53 gene regulation and reduce p53 stability by targeting it for ubiquitination. Overall PBF overexpression reduces DNA repair capacity and induces genetic instability. Figure 4 shows a focused cDNA PCR array examining 84 murine DNA repair or genetic instability genes in wild type and PBF-Tg mice; 17 genes were significantly deregulated. One of these genes was Rad6, with approximately a two fold increase. Protein expression of Rad6 was similarly induced in thyroid glands of PBF-Tg mice (unpublished).

Figure 4.

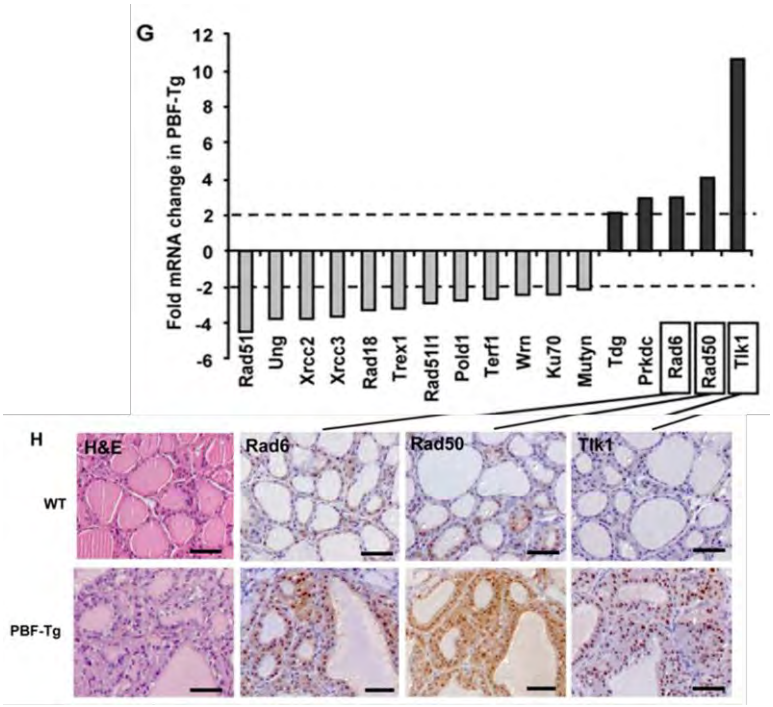

Figure 4. Graph summary from focused cDNA PCR array examining 84 murine DNA repair or genetic instability genes in wild type and PBF-Tg mice. Note Rad6 with an approximately two fold increase in expression. Below are immunohistochemistry examples of thyroid glands from PBF-Tg mice supporting findings of increased protein expression of Rad6 (unpublished).

1.5 Rad6

Like PBF, Rad6 is a small protein (17kDa) whose role is not clearly defined. It has a dual role in DNA repair, involved in both the degradation and transcription of p53. In humans there are two homologues of Rad6 sharing 95% sequence homology; HHR6A and HHR6B. HHR6A is on chromosome Xq24-25 and mutations have led to infertility in females. HHR6B is on chromosome 5.23-q21 and mutations can cause sterility in males. Mice lacking both HHR6A and HHR6B are non-viable (19, 20, 21). Also like PBF, Rad6 sequences are highly conserved throughout species suggesting a functional importance. Although not well characterised, Rad6 is part of a group of E2 enzymes involved in DNA damage and repair. E2 enzymes covalently add ubiquitin to specific lysine residues of substrate proteins. All known functions

of Rad6 result from ubiquitination and when the conserved cysteine 88 is replaced with serine or alanine a null phenotype ensues (19).

Post replication DNA repair occurs after DNA synthesis when unrepaired lesions in the template strand induce stalling of DNA replication causing gaps in the new strand. There are two post replication repair pathways that complete DNA synthesis; error free and error prone and both are regulated by the Rad6 gene (Figure 5). These pathways are both initiated by Rad6's interaction with Rad18 catalysing the monoubiquitination of proliferating cell nuclear antigen (PCNA) on lysine-164 (Figure 5). The error prone pathway involves a mutagenic bypass of damaged sites with a specialised DNA polymerase. Alternatively Rad6 can form a complex with Ubc13, MMS2, Rad5/Rad18 and enter the error free route, bypassing by template switching and/or gap filling by recombination. Rad6 mutations in the catalytic site have shown hypersensitivity to DNA damaging agents (22, 23, 24).

Figure 5.

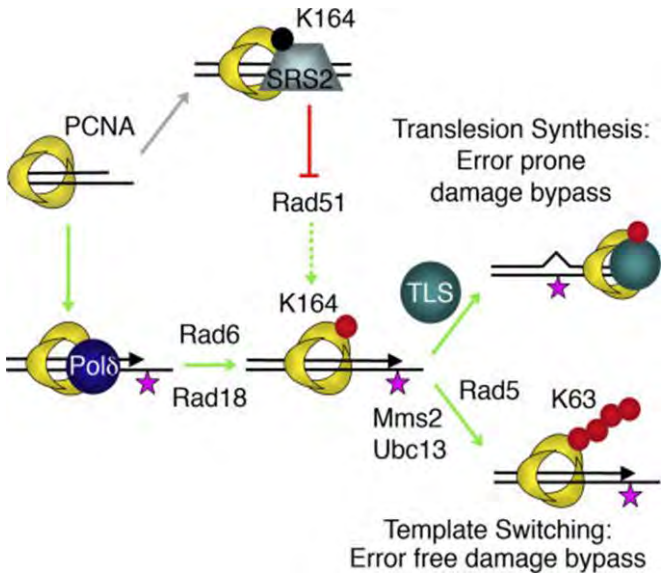

Figure 5. Simplified diagram of Rad6's involvement in DNA repair. Following DNA damage (star) Rad6 forms a complex with Rad18 to monoubiquitinate lysine-164 and then either the error prone or error free pathway will ensue. Translation synthesis (TLS) (24).

As already stated Rad6 has a dual role in p53 regulation; involved in both its degradation and transcription. Normally Rad6 forms a complex with mdm2 to regulate p53 through ubiquitination. However under stress, such as DNA damage, Rad6 is recruited to the promoter and coding regions of the p53 gene and regulates H3K4 and H3K79 methylation levels. In these stress situations the Rad6-mdm2-p53 degradation complex is disrupted and additional Rad6 is recruited to p53 gene chromatin, activating transcription (18, 24).

PBF's effect of increasing Rad6 levels raises many possibilities. Oncogenic expression of PBF leading to the rise in DNA repair proteins, like Rad6, may be due to a direct interaction between PBF and Rad6 transcription. As both PBF and Rad6 can bind to and influence p53, perhaps PBF by raising Rad6 levels, increases p53 degradation via Rad6 polyubiquitination. Higher amounts of Rad6 may also enhance error prone DNA repair. Or, it is possible that the rise of Rad6 is an indirect result of PBF causing high levels of genetic instability and decreased p53 stability. A normal cellular response to such stress would be transcription of p53 and attempting to initiate DNA repair. It is not clear if Rad6 enhances or inhibits PBF effects on tumourigenesis.

2.0 AIMS AND HYPOTHESIS

As PBF appears to induce Rad6 and both PBF and Rad6 are capable of altering the stability of p53 the aim of this project was to determine whether PBF directly impairs DNA repair by the promotion of Rad6 deregulation of p53. The hypothesis is that by inducing Rad6, PBF impairs DNA repair and this interaction could be a potential therapeutic target.

3.0 METHODS

3.1 Cell Culture

TPC-1-1 (papillary thyroid) and K1 (papillary thyroid) cells were cultured in RPMI 1640 supplemented with 1% penicillin-streptomycin and 10% fetal bovine serum (FBS) in T75 flasks. Once 80% confluent, cells were split or seeded. To seed, the media was removed and cells washed in sterile phosphate buffered saline (PBS, 1 tablet/100ml dH_20, Oxoid) before being trypsinised at 37^0C with 0.25% trypsin and re-suspended with RPMI. Cells were counted using a haemocytometer. In 6 well plates TPC-1 cells were seeded at 7.5 $x10^4$ cells per well and K1 cells were seeded at 1 $x10^5$ cells per well.

3.2 siRNA

To achieve knockdown, Rad6 A, Rad6 B and negative control scrambled siRNA (all from Ambion) were diluted to a final concentration of 40µM. 6µl of lipofectamine (Invitrogen) and 1µl of siRNA were used per well of a 6 well plate and made up to 1ml with Optimum media. After 4 hours the Optimum media was replaced with 2mls of RPMI. All knockdowns were for 48 hours prior to protein harvesting.

3.3 Transfection

The quantity of vector only (pcDNA-3), PBF (as described in Stratford et al 2005, 25) and Rad6 (Origene in pCMV6-XL5) were calculated for 2000ng per well of a 6 well plate and 5000ng per T25 flask. Fugene (Roche) was used at 6µl per well of a 6 well plate and 15µl in a T25 flask, to a total of 100µl and 500µl with Optimum media respectively. Transfections were for 24 hours.

3.4 Protein Harvesting

For protein harvesting the media was removed and cells washed with PBS. RIPA buffer with protease inhibitor cocktail (60µl/ml RIPA buffer, Sigma) was applied and cells incubated at -20^{0}C for 20 minutes. After defrosting, plates were scraped and collected into Eppendorfs. To clarify, the samples were centrifuged at 4^{0}C for 10 minutes and the supernatant stored at -20^{0}C. To calculate the yield of protein in mg/ml, BCA Assay (BioRad) was used as per manufacturer's instructions and compared to BSA standards.

3.5 Western Blotting

After BCA Assay the volume of sample required was calculated and added to 4x Laemmli sample buffer (0.106g DTT (Sigma) per 1ml Laemmli sample buffer (Bio Rad)), before being heated to 95^{0}C for 5 minutes. Proteins were separated on a 12% SDS-PAGE gel (Resolving gel: dH_20, Acrylamine (Geneflow), 1.5M Tris, 10% SDS (Sigma), 10% APS (Sigma), Tetramethylethylenediamine (Temed, Sigma); stacking gel: dH_2O, acrylamide, 0.8MTris, 10% SDS, 10% APS, Temed) and then transferred to a PVDF membrane (Sigma). Membranes were blocked in 5% non-fat milk in TBST (dH_20, 1M Tris, NaCl (Fisher), Tween 80 (Sigma)). Antibodies were made up in 5% non-fat milk and TBST. Primary antibodies included PBF used at 1:500 (manufactured in lab), Rad6 1:1000 (0.5mg/ml Ambion), p53 1:1000 (SantaCruz Biotechnology) and β-actin 1:10000 (Sigma). HRP conjugated secondary antibodies were used and included rabbit anti-mouse and goat anti-rabbit (both Dako). Membranes were then developed using ECL pierce (Thermo Scientific) as per manufacturer's instructions on Xograph Compact X4. Densitometry was performed using Image J.

3.6 Co-immunoprecipitation

Cells were grown in T25 flasks and protein harvested as described in sections 3.1 and 3.4. 35µl of the supernatant was collected as lysate and stored at -20^{0}C (15µl of 4x Laemmli sample buffer was added and samples heated to 95^{0}C prior to Western Blotting). Protein G Sepharose beads (GE Healthcare) were prepared as per manufacturer's instructions and added to the remaining sample with antibody (10µl PBF per sample and 10µl Rad6 at 0.5 mg/ml) and spun on a rotating mixer at 4^{0}C for 2-4 hours. Samples were then centrifuged at 4^{0}C, the supernatant was discarded and the beads washed in RIPA buffer before elution buffer was applied (Laemmli buffer, β-mercaptoethanol (Aldrich), 10% SDS). Samples were then heated to 37^{0}C for 30 minutes before centrifugation. The supernatant was then stored at -20^{0}C. The entire sample was used to Western Blot as described in section 3.5.

3.7 Immunofluorescence

Cells were grown on cover slips as described in cell culture. The media was removed and cells washed with PBS. Fixing solution (0.2M phosphate buffer, 0.2M Na2HPO4 corrected to ph7.4, PFA, Glucose, 0.1% sodium azide, dH20) was applied for 20 minutes at room temperature. The fixing solution was then removed and cells washed in PBS. The cells were permeabilised with cooled 100% methanol for 10 minutes at -20^{0}C. The methanol was removed and the cells washed with PBS. To reduce non-specific binding, cells were blocked in 10% normal goat serum/ newborn calf serum (NGS/NCS) for 30 minutes at room temperature. Primary antibodies were prepared in 1% bovine serum albumin (BSA) in PBS (Rad6 1:150, p53 1:200) and incubated for 1 hour. Cells were then washed in PBS. Secondary antibodies were prepared in 1% BSA with 1%NCS, (goat anti-rabbit and goat anti-mouse used at 1:250 (Invitrogen), Hoescht stain 1:1000) and incubated in the dark for 1 hour. Cells were washed again in PBS and slides mounted using fluorescent mounting medium

(Dako) and sealed with nail varnish. Coverslips were allowed to dry and stored in the dark at -4^{0}C. Once dry, slides were imaged and captured on a Zeiss Axioplan fluorescent microscope (Zeiss, Germany).

3.8 Mutagenesis

Mutagenesis was carried out using Stratagene one step mutagenesis kit as per manufacturer guidelines. Primers were designed and ordered from Alta Bioscience to mutate cysteine 88, a known ubiquitination site for Rad6, to an alanine (forward 5'GCA-GAT-GGT-AGT-ATA-GCT-CTG-GAC-ATA-CTT-CAG-AAC-CGT-TG 3', reverse 5' CG-GTT-CTG-AAG-TAT-GTC-CAG-AGC-TAT-ACT-ACC-ATC-TGC 3'. After growing on agar plates, colonies were selected for sequencing and analysed using Chromas.

3.9 Statistical Analysis

Data were compared by student's t-test method to determine statistical significance. Results are expressed as mean ± standard deviation. A p value <0.05 was deemed significant.

4.0 RESULTS

4.1 Rad6 siRNA reduces p53 protein levels. PBF reduces p53 stability and increases Rad6 levels two fold (Figure 4). Rad6 can have a dual effect on p53 expression dependent on cell stress. The impact of manipulating Rad6 expression on p53 was measured to determine if this was concordant or counteractive with PBF's influence. TPC-1 cells were treated with siRAD6 A, B or Rad6 A and B combined (Rad6 AB) with Scrambled siRNA as negative control. Harvested protein from the treated cells were separated by SDS-PAGE and the subsequent blots probed for Rad6, p53, PBF and β-actin. Unfortunately PBF was undetectable and Rad6's effect on p53 was variable. siRad6 A alone did deplete Rad6 and significantly lowered p53 levels (p=0.02, Figure 6A and B). However, siRad6 B had no significant impact on either Rad6 or p53 (p=0.54 and p=0.12 respectively, Figure 6A and B). siRad6 AB did appear to lower p53 levels, but the result was short of significane (p=0.08, Figure 6C and D). It should be noted that although Rad6 A and B can be seperately knocked down using siRNA, the Western blot antibody detects the combined protein levels for the Rad6 homologues.

Figure 6. (A)

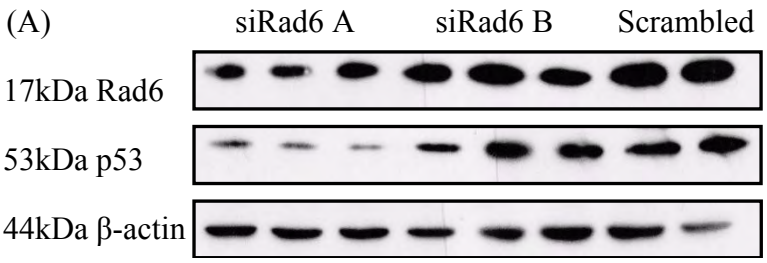

(B)

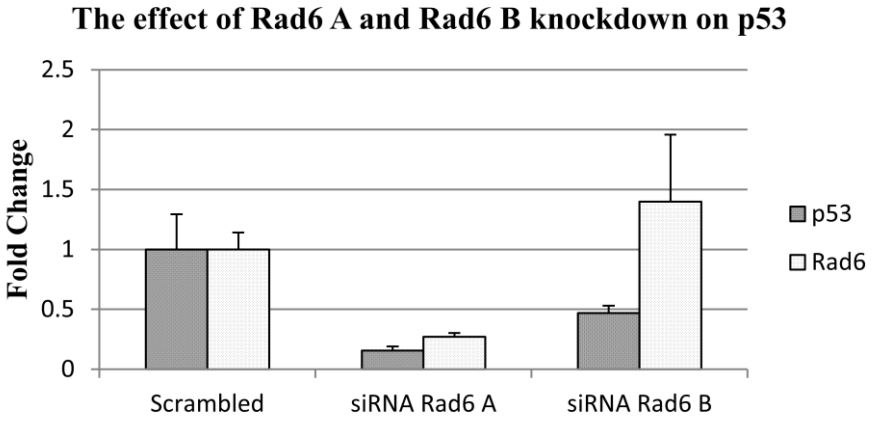

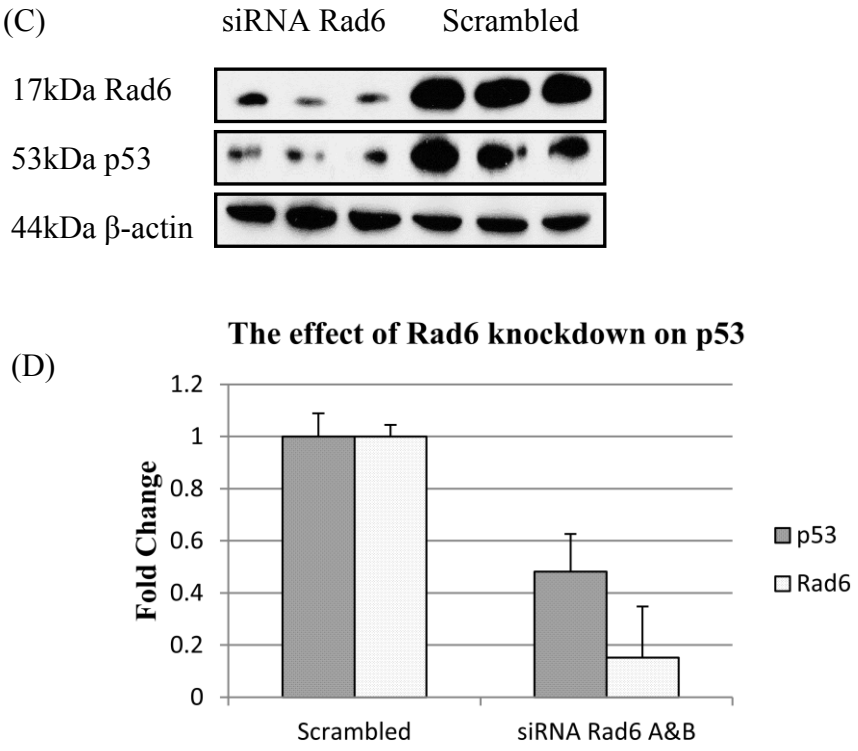

Figure 6. TPC-1 cells were depleted of Rad6 A, B or A and B combined using siRNA for 48 hours. Harvested protein were separated by SDS-PAGE and subsequent blots were probed for p53, Rad6 and β-actin. Densitometry was performed using Image J and significance was determined using student's paired, two-tailed t-test. (A) An example of a Western blot of siRNA Rad6 A and Rad6 B. (B) Densitometry of siRNA Rad6 A and Rad6 B effect on p53 and Rad6 when compared to β-actin (N=2). Rad6 A significantly reduced p53 (p=0.02). Rad6 B siRNA did not significantly reduce levels of Rad6 or p53 (p=0.54 and p=0.12 respectively). (C) Western blot with siRNA Rad6 AB. (D) Densitometry graph comparing p53 and Rad6 against β-actin (N=4). Good delpetion of Rad6 was achieved (p=0.015). However the fall in p53 was not significant (p=0.08).

4.2 Rad6 siRNA reduces p53 levels in the stressed cell. Rad6 knockdown lowered p53 levels (Figure 6) under normal conditions and to determine if this also occurred under p53 stimulating situations of the stressed cell, TPC-1 cells were exposed to 15Gy irradiation after 48 hour knockdown of Rad6 AB with scrambled siRNA was used as negative control. In scrambled irradiated cells p53, as expected, increased and was not induced in control samples (Figure 7). Although p53 levels rose with irradiation after siRad6 AB treatment, this was not as considerable as that of control (Figure 7). PBF appeared at 25kDa or around 34kDa in a glycosylated form. Overall the levels of PBF did not vary with irradiation.

Figure 7.

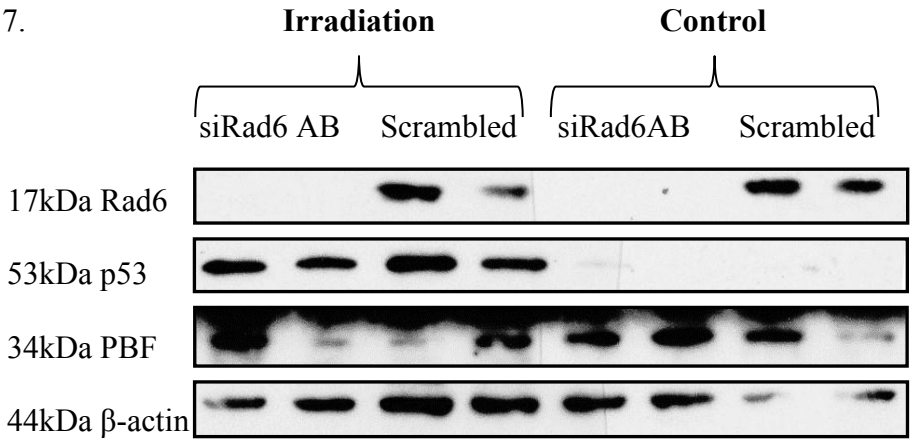

Figure 7. TPC-1s were depleted of Rad6 A and B using siRNA for 48 hours and then exposed to 15Gy irradiation. Control cells were not exposed to irradiation. Protein was harvested and separated by SDS-PAGE before blots were probed for p53, Rad6, PBF and β-actin (N=3).

4.3 Rad6 and PBF may not bind in complex. PBF overexpression leads to an increase in Rad6 levels (Figure 4). However, Rad6 knockdown did not have a reciprocal effect on PBF (Figure 7). PBF and Rad6 can both separately form a complex with p53 and so to determine if Rad6 and PBF bind in complex co-immunoprecipitation experiments were performed. Both K1s and TPC-1s were used with and without PBF transfection. Rad6 antibody was used to pull-down for PBF (Figure 8A and B) and in separate experiments, PBF antibody was used to pull-down for Rad6 (Figure 8C and D). No binding was found between Rad6 and PBF (N=2).

Figure 8. Co-immunoprecipitation.

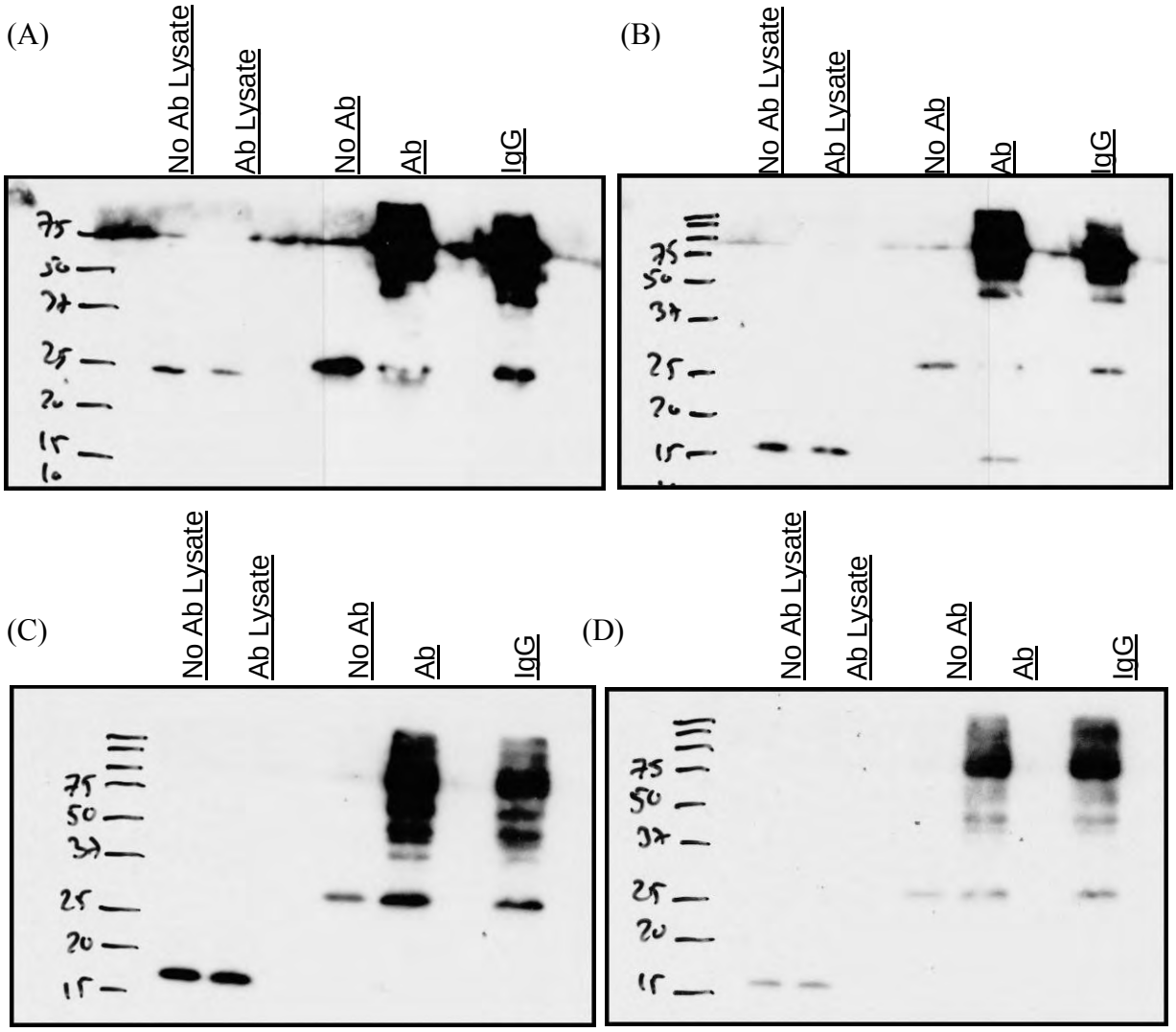

Figure 8. TPC-1 and K1 cells were harvested for co-immunoprecipitation. Rad6 or PBF antibody were added to the harvested lysate and protein G Sepharose beads before being spun on a rotating mixer. The supernatant was discarded and elution buffer applied to the beads and antibody-protein complexes. Samples were then separated by SDS-PAGE and blots probed for PBF and Rad6. Rad6 antibody was used to pulldown for PBF and PBF antibody was used to pulldown for Rad6. (A) Rad6 antibody (Ab) pulldown for PBF. (B) Rad6 antibody pulldown for Rad6. (C) PBF antibody pulldown for Rad6. (D) PBF antibody pulldown for PBF. No binding between PBF and Rad6 can be seen.

4.4 Rad6 overexpression induces PBF. PBF raises Rad6 levels approximately two-fold (Figure 4). To replicate this and uncover if increased Rad6 could influence PBF levels, Rad6 or PBF was transfected into TPC-1s and K1s. PBF overexpression was not successful and so

the data could not be confidently interpreted. However, Rad6 overexpression was consistent. Increasing Rad6 had no effect on p53 levels, but interestingly increased PBF (Figure 9).

Figure 9.

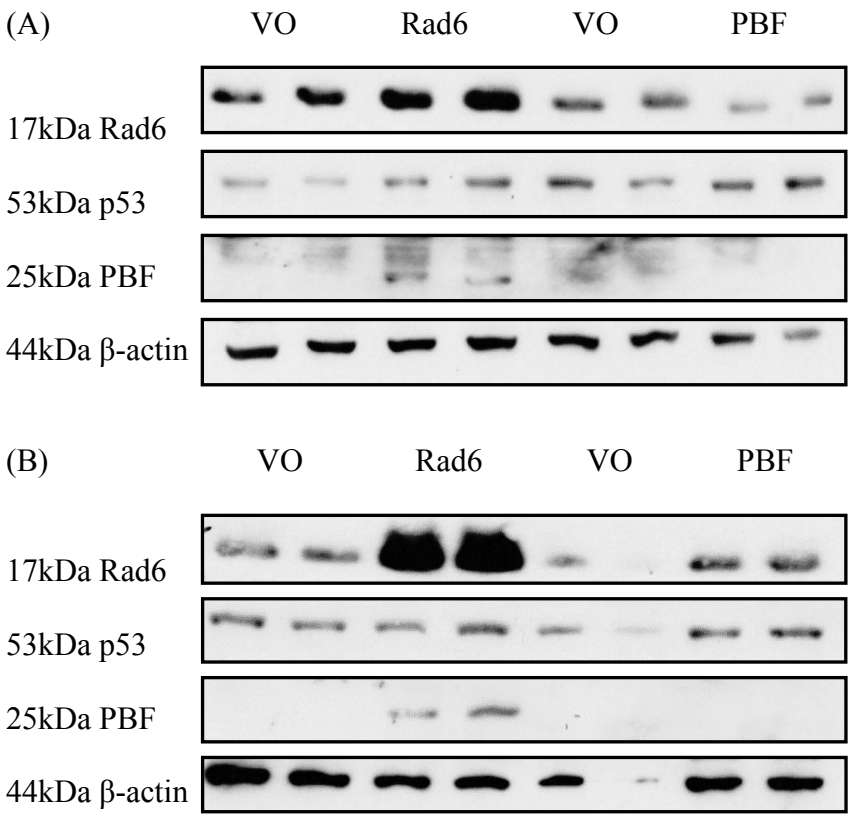

Figure 9. TPC-1 and K1 cells were transfected with Rad6, PBF, or vector only (VO) control for 24 hours. Protein was then harvested and separated by SDS-PAGE. Blots were probed for Rad6, PBF, p53 and β-actin. TPC-1s N=2, K1s N=3. (A) Example of Western blot after Rad6, PBF and VO transfection in TPC-1 cells and the effect on Rad6, p53 and PBF. (B) Example of Western blot after Rad6, PBF and VO transfection in K1 cells and the effect on Rad6, p53 and PBF.

4.5 Rad6 knockdown inhibits p53 rise in stressed cells. Ideally in order to ascertain the complex interaction between PBF, Rad6 and p53, visualisation using immunofluorescence under differing circumstances would be attempted; siRad6, Rad6 transfection, PBF transfection, with and without irradiation. Any co-localisation occurring could then be identified and under what circumstances. Unfortunately however, both PBF and Rad6 antibodies are anti-rabbit and no other immunofluorescence antibody preparations are

currently available for Rad6. PBF antibody with HA tag is anti-mouse, but evidence suggests that it can interfere with PBFs ability to enter the nucleus (unpublished). Due to these difficulties Rad6 and PBF were not visualised together, instead Rad6's influence on p53 was explored. Cells were treated with siRad6 AB, scrambled siRNA, Rad6, or vector only and either were, or were not exposed to 15Gy irradiation. Figure 10A and B support Western blot findings shown in Figure 9, whereby overexpression of Rad6 did not affect p53 levels, however, co-localisation with p53 was apparent. Figure 10C and D also support Western blot findings in Figure 6 and 7; siRNA Rad6 AB lowered p53 levels both with and without irradiation. However, under these conditions there was no co-localisation between p53 and Rad6. Also, after irradiation and Rad6 transfection, p53 was located more in the cytoplasm (Figure 10B ad D).

Figure 10.

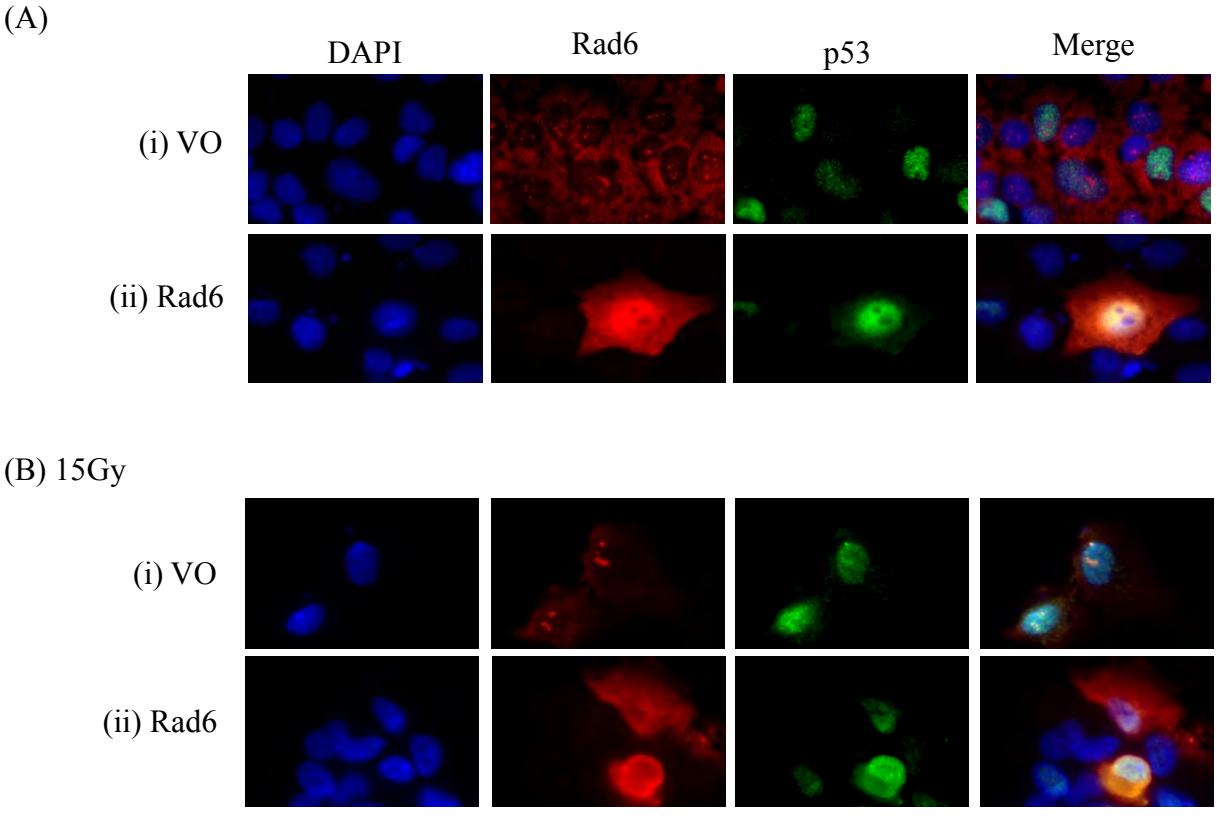

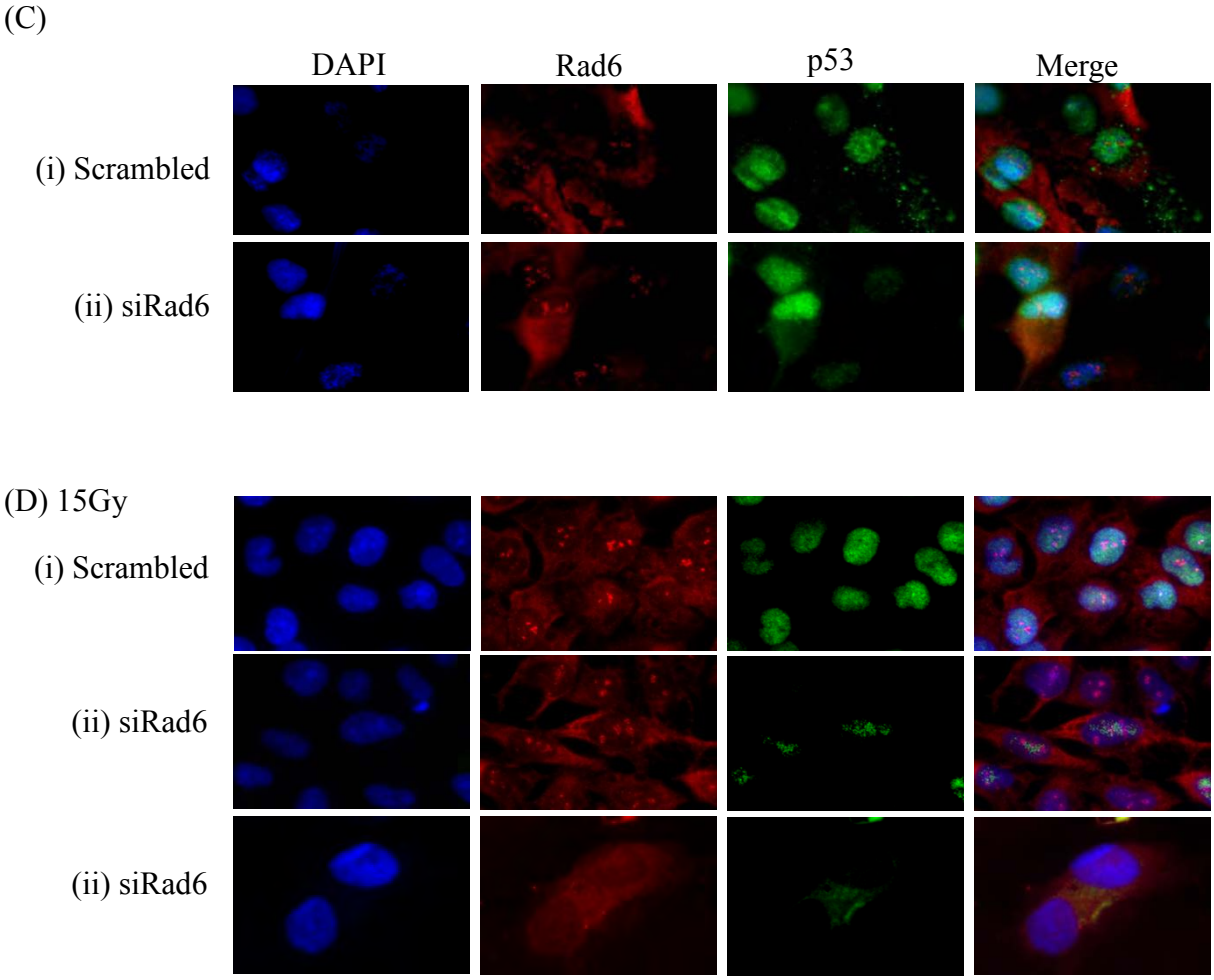

Figure 10. TPC-1s and K1s were transfected with Rad6 or vector only (VO) control for 24 hours, siRNA Rad6 AB or scrambled for 48 hours and either exposed or not exposed to 15Gy irradiation. Slides were fixed and stained with Rad6 and p53 primary antibody followed by appropriate fluorescent secondary antibodies (Rad6 in Red and p53 in Green) and Hoescht stain (blue). Slides were imaged at 100x magnification. (A) TPC-1s (i) Vector only control (ii) Rad6 overexpression. (B) K1s after exposure to irradiation (i) Vector only control (ii) Rad6 overexpression. (C) K1s (i) Scrambled (ii) siRad6 AB. (D) TPC-1s after exposure to irradiation (i) Scrambled (ii) siRNA Rad6 AB (iii) K1s after exposure to irradiation siRNA Rad6 AB.

5.0 DISCUSSION

Using HeLa and HCL-7702 cells, Chen et al. (18) demonstrated that neither knockdown nor overexpression of Rad6 had an effect on p53 protein levels. They did show, however, that siRNA directed towards Rad6 A, B or AB combined resulted in a reduction in p53 mRNA. This effect was more significant in Rad6 A and Rad 6 AB knockdown compared to Rad6 B, suggesting that Rad6 A has the greater impact on p53. Although there is siRNA against each Rad6 homologue, Western blot antibodies are unable to distinguish between Rad6 A and Rad6 B. In an attempt to understand how Rad6 influences p53 and PBF levels in thyroid cancer, siRNA directed towards Rad6 was used in TPC-1 cells. Knockdown was achieved with Rad6 A and Rad6 AB (Figure 6). Interestingly with Rad6 B siRNA there was no significant change in Rad6; this was not found in other studies and may be related to the cell line used. It is possible that in response to Rad6 B depletion, Rad6 A is up-regulated and this is what was detected by the antibody. Alternatively, Rad6 B may account for only a small proportion of total Rad6 in TPC-1 cells, with depletion leading to negligible differences in overall Rad6 levels. This emphasises the lack of characterisation of Rad6 and the role of each homologue. p53 levels are tightly controlled by many pathways and when comparing p53 protein levels in siRad6 and control, p53 appeared to be reduced by all knockdowns of Rad6. However, densitometry for siRNA against Rad6 AB was not significant (Figure 7, $p=0.08$, $N=4$). With greater numbers this may be achieved. Depletion with siRNA Rad6 A alone did however significantly reduce p53 protein levels (Figure 7, $p=0.02$, $N=2$). However with low repeats ($N=2$) this work requires further study. It is not clear why depleting only one form of Rad6 would have a greater impact than dual knockdown on p53 protein levels. According to research by Chen et al (18), Rad6 does have a “ying yang” effect on p53, being involved in both its degradation and transcription. Both the degradation and transcription of p53 will be occurring simultaneously and it is the equilibrium that will shift under certain conditions. By

depleting Rad6, other pathways are likely to influence p53 to maintain appropriate cellular concentrations. When both Rad6 homologues are knocked down this could act as a trigger for the other pathways to maintain p53 levels. The alteration in p53 levels may also be cell line related. TPC-1s were chosen as they are a thyroid cancer cell line with wild type p53. Read et al (unpublished) have found that PBF reduces p53 stability. As Rad6 also affects p53 levels, PBF was probed for in the siRad6 experiments discussed above, although no clear bands were visible. This may be a reflection on the antibody's inability to detect small amounts of PBF.

As Rad6's known functions relate to ubiquitination and are dependent on cysteine 88, mutagenesis was attempted to convert cysteine 88 to an alanine for a null phenotype. The mutant Rad6 would then be transfected into cells and the impact on p53 and PBF ubiquitination observed. Unfortunately, the resulting colonies selected for sequencing showed wild type Rad6. Rad6 B knockdown experiments showed that either Rad6 B is a minor protein in TPC-1 cells or that Rad6 A can be up-regulated. There was concern that as only Rad6 A variant 1 would have been mutated, wild type Rad6 B may be up-regulated to perform Rad6 functions. This would be interesting to research and aid further characterisation of Rad6 and the roles of each homologue. However, due to time constraints and as Rad6 knockdown was consistently achieved siRNA was used under various conditions instead of optimising mutagenesis.

Under stress from DNA damage, such as that from irradiation, p53 is stabilised (26). PBF has been shown to increase genetic instability and survival in response to irradiation, while also reducing p53 stability (unpublished observation). TPC-1 cells with depleted Rad6 AB were irradiated with 15Gy and the effect on p53 and PBF measured. In control experiments p53 was increased with no apparent rise in Rad6 levels (Figure 7). As described by Chen et al (18), under cell stress Rad6 is released from the ternary complex with p53 and mdm2, then

recruited to chromatin to methylate histones and trigger p53 transcription. There is not an overall increase in Rad6, but an alteration in function. p53 levels were lower with Rad6 knockdown even with irradiation stimulus, implying Rad6 knockdown can deplete p53. Surprisingly PBF levels appeared unchanged throughout. Work within the lab (unpublished) had found that PBF did not affect p53 mRNA levels, indicating the reduction in p53 stability was a post translational effect. Chen et al (18) also knocked down Rad6, finding that the up-regulation of p53, induced by doxorubicin treatment in HeLa cells, was inhibited. Similarly to results in Figure 6, they did not find this with Rad6 B knockdown.

PBF and Rad6 are both raised in cancer and can influence p53 levels. Both have also been shown to separately bind p53 (17, 18, unpublished). To discover if Rad6 and PBF also bind, perhaps with p53 in complex, co-immunoprecipitation was performed. TPC-1s and K1s, with and without overexpressed PBF, were used with PBF pull down for Rad6 and Rad6 pull down for PBF. The experiments were a technical challenge and often unsuccessful. They did not show any binding between Rad6 and PBF, however PBF was difficult to detect on Western blot; perhaps due to low levels (Figure 8). With reference to the next experiments involving Rad6 overexpression, Rad6 transfection prior to co-immunoprecipitation may be more successful in determining if PBF and Rad6 bind in complex.

With oncogenic expression of PBF, Rad6 is increased two fold both *in vitro* and *in vivo* (unpublished, Figure 4.) To observe if Rad6 influenced PBF levels in a reciprocal fashion TPC-1s and K1s were transfected with Rad6, PBF or vector. The harvested protein was separated by SDS-PAGE and probed for PBF, Rad6 and p53. Rad6 was in vector pCMV6-XL5 and PBF in pcDNA-3, the control vector used was pcDNA-3 only. Although not an ideal control, pCMV6-xl5 is of similar size and nature. Rad6 transfection led to consistent overexpression, unfortunately PBF did not. Antibody directed towards p53 revealed no change in protein levels with Rad6 overexpression. In both cell lines overexpressed Rad6

raised PBF protein levels (Figure 9, TPC-1 N=2, K1 N=3). Therefore Rad6 and PBF can influence each other's protein levels. Understanding the influence of Rad6 knockdown on PBF levels and subsequent co-immunoprecipitation experiments will be essential in understanding the interaction.

A visual analysis would aid understanding of Rad6 and PBF's relationship. However, this was not possible as Rad6 primary antibody is rabbit, with no alternative antibody preparations being available. PBF primary antibody is also rabbit, unless with HA tag. The HA tag however, can alter PBF behaviour and inhibit PBF's ability to enter the nucleus (unpublished). Instead, TPC-1s and K1s were transfected with Rad6, vector only, siRNA Rad6 AB or scrambled, then being either irradiated or not were imaged for Rad6 and p53. On imaging, not all cells survived and so there were incomplete results for TPC-1s and K1s separately. Images of controls revealed similar results to that seen by Shekhar et al (28); Rad6 formed foci in the nucleolus, but was predominantly in the cytoplasm and p53 was generally confined to the nucleus without any co-localisation (Figure 10 A and C). Under normal circumstances Rad6 that co-localises with p53 (Rad6-p53-mdm2 complex) leads to p53 degradation and so little will be visualised together. These findings support Chen et al (18), who demonstrated that Rad6 forms ternary complexes with p53 and mdm2 under normal conditions, but did not observe this in immunofluorescence. Lyakhovich and Shekhar (19) found after DNA damage Rad6 forms supramolecular complexes with p53 and p14ARF, correlating with p53 stability, but they did not demonstrate any co-localisation. Figure 10 A and B show only overexpressed Rad6 co-localised with p53 and was more diffuse throughout the nucleus and cytoplasm, with no foci in the nucleolus and as Western blots demonstrate in Figure 9 the overall levels of p53 were unchanged. These findings contrast with Chen et al (18). They imaged H1299 cells overexpressing Rad6 A or B and found that this promoted the cytoplasmic localisation of p53 with no obvious co-localisation. There is now conflicting data

as to whether over expressed Rad6 does co-localise with p53. Protein levels of Rad6 did not rise in response to irradiation (Figure 8). Therefore the transfected Rad6 which co-localised with p53 may be representative of oncogenic Rad6 as seen with PBF and not reflective of Rad6 behaviour under normal conditions. In support of this hypothesis Shekhar et al (28, 29) did observe an increase of Rad6 B in tumours and found an imbalance of Rad6 (as that perhaps seen with PBF) can lead to chromosomal instability and transformation.

The aim of this project was to determine whether PBF directly impairs DNA repair by promoting Rad6, thus leading to p53 deregulation. Rad6's relationship with p53 is complex and transfection of Rad6 to oncogenic levels increased PBF, but did not alter p53 levels (Figure 9). It does however lead to Rad6 co-localising with p53, which was not seen under normal conditions (Figure 10A and B). Therefore overexpressed Rad6 may lead to p53 deregulation. In addition, Rad6 depletion lowered p53 protein levels, even under p53 stimulatory conditions, with no effect on PBF protein levels (Figure 6, 7, 10C and D). Further work is clearly needed to uncover if PBF is impairing DNA repair through the promotion of Rad6 and deregulation of p53. How oncogenic Rad6 effects DNA repair could be measured, using, for example, Comet assays. Co-immunoprecipitation with transfected Rad6 cells for pull-down of PBF may reveal PBF and Rad6 do form a complex, implying PBF is directly interacting with Rad6. In addition, mutagenesis with C88A and examining both protein and mRNA levels of p53 may help understand how Rad6 A and Rad6 B levels effect each other and if Rad6 A and Rad6 B have different effects on PBF. There is a complex relationship between PBF, Rad6 and p53, which is consequently difficult to understand as both PBF and Rad6 have yet to be fully characterised.

REFERENCES

1. NHS Choices (2010). Thyroid Cancer (02/08/2012). http://www.nhs.uk/conditions/Cancer-of-the-thyroid/Pages/Introduction.aspx
2. Nussey S, Whitehead S. Endocrinology: An Integrated Approach. Oxford: BIOS Scientific Publishers; 2001. Chapter 3, The thyroid gland. Available from: http://www.ncbi.nlm.nih.gov/books/NBK28/
3. Miller RJ. (2012). Thyroid Anatomy (02/08/2012). http://www.aboutcancer.com/ThyroidAnterior_907.gif
4. Healthy body network (2010). The Anatomy of the Thyroid Gland (02/08/2012). http://www.painneck.com/thyroid-gland-anatomy
5. Ali S. BMJ Evidence Centre (2011). Thyroid hormone production (02/08/2012). http://bestpractice.bmj.com/best-practice/monograph/1121.html
6. World Health organisation (2006). Health effects of the Chernobyl accident: an overview (02/08/2012). http://www.who.int/mediacentre/factsheets/fs303/en/index.html
7. Boice JD. Thyroid disease 60 years after Hiroshima and 20 years after Chernobyl. *JAMA*. 2006; 295(9): 1060-1062.
8. Cancer research UK (2012). Thyroid cancer (02/08/2012) http://cancerhelp.cancerresearchuk.org/type/thyroid-cancer/
9. Jones MK. Management of papillary and follicular thyroid cancer. *JRSM*. 2002; 95(7). 325-326.
10. ThyCa: Thyroid Cancer Survivors' Association, Inc. (2011). Facts about thyroid cancer (02/08/2012). http://www.thyca.org/thyroidcancerfacts.htm
11. Smith VE, Franklyn JA, McCabe CJ. Pituitary tumor-transforming gene and its binding factor in endocrine cancer. *Expert Rev Mol Med*. 2010; 12, e38.
12. Kim D, Pemberton H, Stratford A, Buelaert K, Watkinson JC et al. Pituitary tumour transforming gene (PTTG) induces genetic instability in thyroid cells. *Oncogene* 2005; 24: 4861-4866.
13. Chen W, Pei L. A Novel Binding factor Facilitates Nuclear Translocation and transcriptional Activation Function of the Pituitary Tumor-transforming Gene Product. *J Biol Chem*. 2000; 275(23): 19422-19427
14. Stratford AL, Boelaert K, Tannahill LA, Kim DS, Warfield E et al. Pituitary tumor transforming gene binding factor: a novel transforming gene in thyroid tumorigenesis. *J Clin Endocrinol Metab*. 2005; 90: 4341-4349.
15. Boelaert K, Smith VE, Stratford AL, Kogai T, Tannahill LA et al. PTTG and PBF repress the human sodium iodide symporter. *Oncogene*. 2007; 26: 4344-4356.
16. Smith VE, Read ML, Turnell AS, Watkins RJ, Watkinson JC et al. A novel mechanism of sodium iodide symporter repression in differentiated thyroid cancer. *J Cell Sci*. 2009; 122: 3393-3402.
17. Read ML, Lewy GD, Fong JCW, Sharma N, Seed RI et al. Proto-oncogene PBF/PTTG1IP Regulates Thyroid Cell Growth and Represses Radioiodine Treatment. *Cancer Res*. 2011; 71: 6153-6164.
18. Chen S, Wang DL, Liu Y, Sun FL. RAD6 Regulates the Dosage of p53 by a Combination of Transcriptional and Posttranscriptual Mechanisms. *Mol Cell Biol*. 2012; 32(2): 576-587.
19. Lyakhovich A, Shekhar MPV. Supramolecular Complex Formation between Rad6 and Proteins of the p53 Pathway during DNA Damage-Induced Response. *Mol Cell Biol*. 2003; 23(7): 2463-2475.

20. Roest HP, Baarends WM, de Wit J, van Klaveren JW, Wassenaar E et al. The ubiquitin-conjugating DNA repair enzyme HR6A is a maternal factor essential for early embryonic development in mice. *Mol Cell Biol*. 2004; 24: 5485-5489
21. Roest HP, van Klaveren J, de Wit J, van Gurp CG, Koken MH et al. Inactivation of the HR6B ubiquitin-conjugating DNA repair enzyme in mice causes male sterility associated with chromatin modification. *Cell*. 1996; 86: 799-810
22. Lawrence C. The RAD6 DNA repair pathway in *Saccharomyces cerevisiae*: what does it do, and how does it do it? *Bioessasys*. 1994; 16: 253-258
23. Lawrence CW, Hinkle DC. DNA polymerase zeta and the control of DNA damage induced mutagenesis in eukaryotes. *Cancer Surv*. 1996; 28: 21-31.17 ref 30, 31
24. Langerak P, Nygren AOH, Krijger PHL, van den Berk PCM, Jacobs H. A/T mutagenesis in hypermutated immunoglobulin genes strongly depends on $PCNA^{K164}$ modification. *J Exp Med*. 2007; 204(8): 1989-1998.
25. Stratford AL, Boelaert K, Tannahill LA, Kim DS, Warfield A et al. Pituitary Tumour Transforming gene Binding Factor: A Novel transforming Gene in Thyroid Tumorigeneis. *J Clin Endocrinol Metab*. 2005; 90(7): 4341-4349
26. Levine AJ. p53, the Cellular Gatekeeper for Growth and Division. *Cell*. 1997; 88: 323-331.
27. Van Staveren WCG, Weiss Solís DY, Hébrant A, Detours V, Dumont JE et al. Human cancer cell lines: Experimental models for cancer cells in situ? For cancer stem cells? *Biochim Biophys Acta*. 2009: 92-103.
28. Shekhar MPV, Lyakhovich A, Visscher DW, Heng H, Kondrat N. Rad6 Overexpression Induces Multinucleation, Centrosome Amplification, Abnormal Mitosis, Aneuploidy, and Transformation. *Cancer Res*. 2002; 62: 2115-2124.
29. Shekhar MPV, Tait L, Gerard B. Essential Role of T-cell factor/β-Catenin in Regulation of Rad6B: A Potential Mechanism for Rad6B Overexpression in Breast Cancer cells. *Mol Cancer Res*. 2006; 4: 729-745.

Project 2

OESTROGEN METABOLISM IN COLORECTAL CANCER

This project is submitted in partial fulfilment of the requirements of the MRes.

ABSTRACT

Colorectal cancer (CRC) is a worldwide problem which is often asymptomatic in the early stages leading to delayed diagnosis. Unfortunately advanced disease has no cure with treatment being palliative only. Evidence is accumulating that sex hormones can act both as a risk factor and propagate CRC tumour growth. However, current research examining the oestrogen metabolism pathway in CRC has revealed conflicting results. In an attempt to uncover what drives tumour growth the key oestrogen enzymes in both CRC cell lines and human tissue were investigated using LC/MS, FACS, RT-PCR, Western Blotting and radiolabelled steroid sulphatase (STS) activity assay. Results demonstrated that CRC cell line data are extremely variable. Colo205 cells had greatest STS activity within CRC cell lines and in contrast to other studies oestradiol had no effect on apoptosis. In human female samples STS activity was increased in cancerous tissue compared to matched normal controls and this activity could be inhibited by STX64. In conclusion sex hormones are involved in the development and growth of colorectal cancer and STS inhibitors may benefit females with colorectal cancer.

1.0 INTRODUCTION

Colorectal cancer (CRC) is one of the three most common cancers in both men and women, with global figures from 2008 showing 600,000 people succumbing to the disease (1). Geographically the incidence of CRC varies and it was Berg almost 40 years ago that noted CRC was higher amongst descendants from traditionally low-risk populations after moving to developed countries and adopting a Western diet (2). For example, in China CRC rates are low, whereas Chinese Americans in California have very high rates (3). Estimates suggest that 57% of male and 52% of female CRCs are due to lifestyle and environmental factors such as diet, obesity and lack of exercise (1). About 20% of CRCs are due to hereditary causes, including familial adenomatous polyposis, which is often due to a mutation in the APC gene and hereditary non-polyposis colorectal cancer, involving genes in the DNA mismatch repair pathway (2). CRC incidence is also strongly related to age. In the UK between 2007-2009 72% of cases were in those aged over 65 (1).

As with all cancers, survival is related to the stage and grade of disease upon diagnosis. CRC severity is measured using tumour, lymph node, metastasis (TNM) staging and Duke's classification. How these two methods compare is shown in Table 1 (4, 5).

Table 1.

TNM Classification (American Joint Commission on Cancer)				Dukes' Classification
Stages	T	N	M	Stages
Stage 0	Tis	N0	M0	
Stage I	T1	N0	M0	A
	T2	N0	M0	B1
Stage II	T3	N0	M0	B2
	T4	N0	M0	B2
Stage III	T1, T2	N1 or N2	M0	C1
	T3, T4	N1 or N2	M0	C2
Stage IV	Any T	Any N	M1	D

Table 1. Table comparing the tumour, lymph node, metastasis (TNM) and Duke's classification system for staging colorectal cancer (5)

Surgical removal of CRC is the mainstay of treatment, plus, depending on stage, adjuvant chemotherapy and radiotherapy. In addition monoclonal antibodies, such as Cetuximab, can be used to prolong life in advanced CRC with liver metastases (6). When detected in the very early stages, like Duke stage A, CRC 5 year survival is 93%, however if diagnosed at an advanced stage, this falls to just 7% (1). The majority of CRCs arise from asymptomatic pre-existing adenomatous polyps or adenomas. Estimates predict over 5-10 years 5% of adenomatous polyps transform to malignancy by progressive accumulation of genetic mutations, with symptoms usually only once the CRC has advanced (7). As current treatment is most effective in early stage disease, the UK National Health Service (NHS) introduced a bowel screening programme, aiming to detect asymptomatic patients and pre-malignant polyps. First introduced in England in 2006 and by 2010 available throughout the UK, the test involves screening for faecal occult blood every two years and if positive, is followed by colonoscopy. It is predicted that over the next 20 years there could be 20,000 fewer deaths if just 60% of those eligible took part in screening (1).

1.1 Hormones in Colorectal Cancer

30% of all cancers are hormone sensitive and endocrine treatments have subsequently substantially improved life expectancy e.g. breast and prostate cancer. Unfortunately, the influence of hormones on CRC is complex. Evidence suggests sex hormones correlate with frequency and aggressiveness of CRC, but this relationship is ambiguous. A close association exists between breast cancer occurrence and CRC mortality, implying a common aetiological factor. Also, in men CRC and prostate cancer occur together more often than expected (8, 9).

Sex hormones have a range of effects on gastrointestinal physiology. For example, estradiol (E2) can increase gastrointestinal motility in animal models and stimulate normal colonic epithelium and tumour growth in mice (10, 11). In addition oophorectomy leads to colonic

crypt atrophy (12). In 1969 it was noted that nuns have a higher incidence of colorectal cancer than the general population. As nuns do not have children and so uninterrupted menstrual cycles, they have a higher lifetime exposure to oestrogen (13). Supporting this observation it was also found that pregnancy lowers the risk of colorectal cancer (14). It was hypothesised however, that this may not be a direct hormonal influence, but pregnancy altering carcinogenic hepatic bile acid secretions (15). As described above, there are dietary risk factors for CRC and consuming a Western diet and CRC raises carcinogenic secondary bile acid (BAs) levels, mainly deoxycholic acid and lithocholic acid. These BAs exert their effects on the colon through DNA oxidative damage, inflammation and increased cell proliferation. BAs usually cause apoptosis and resistance to BAs induced apoptosis is linked with CRC (2). Overall reproductive factors such as parity, age of having first child, age of menarche and menopause are linked with CRC, strongly suggesting, as with breast cancer, that lifetime oestrogen exposure is an important risk factor (15).

The colon can also encounter oestrogenic compounds exogenously through diet e.g. plant derived phytoestrogens and fungi-mycoestrogens. Countries with diets comprising higher levels of phytoestrogens have lower incidences of breast, prostate and colon cancer (16). The Women's Health Initiative (WHI) conducted a large trial investigating hormone replacement therapy (HRT) and incidence of disease, the results of which showed that HRT lowered CRC occurrence (17). A reduction in CRC rates due to exogenous oestrogen appears at first to conflict with the findings above, whereby higher lifetime oestrogen exposure is associated with an increased risk of CRC. However, it may highlight differences between endogenous and exogenous oestrogen, the latter having a protective influence. Exogenous oestrogenic compounds are directly exposed to the gut, through oral tablets or diet, and can interact with and subsequently alter the local colonic environment.

1.2 Oestrogen Metabolism in the Colon

Hormone dependent tissues produce oestrogen locally, from circulating inactive steroids via the aromatase or sulphatase pathways as outlined in Figure 1. Peripheral conversion of androstenedione to estrone (E1) results in biologically active oestrogen. Hydrophobic oestrogens e.g. E1, can be converted to hydrophilic oestrogens, such as estrone sulphate (E1-S), by oestrogen sulphotransferase (EST/SULT1E1) as shown in Figure 1. Oestrogen sulphates have a low affinity for the oestrogen receptor (ER) and are considered biologically inactive. E1-S circulates bound to albumin at higher concentrations than E1 and E2, suggesting that E1-S acts as a reservoir for biologically active oestrogens. Once de-sulphated, E1 can be further reduced by 17β-hydroxysteroid dehydrogenase type 1 (17β-HSD-1) to E2, which has the highest binding affinity with ER (18, 19, 20).

Figure 1.

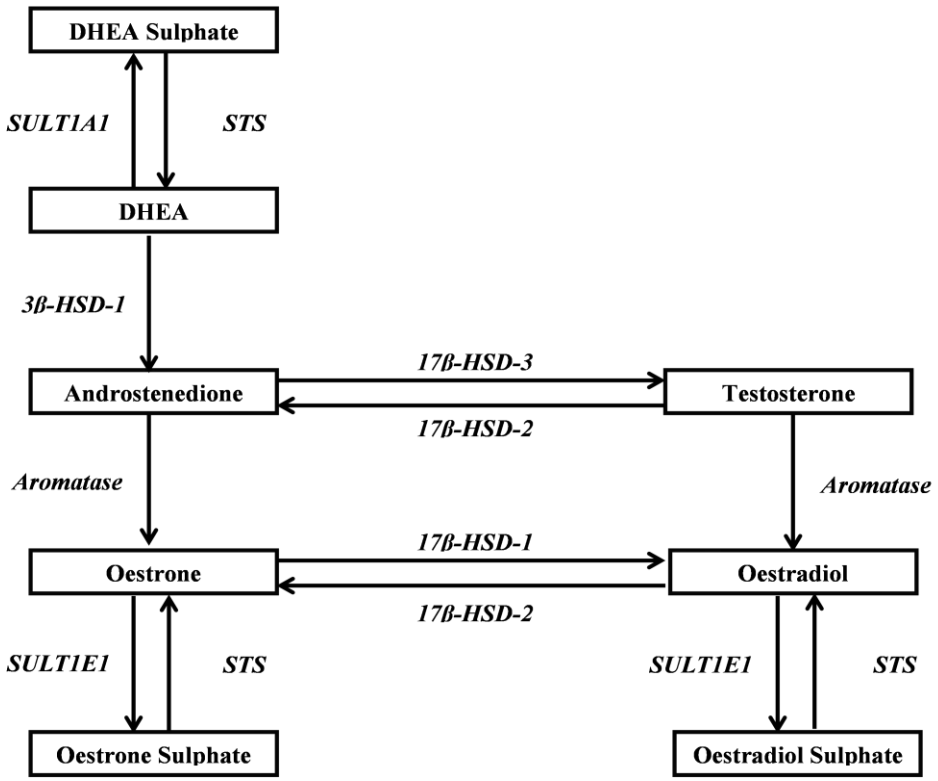

Figure 1. Flow diagram of the oestrogen metabolism pathway. DHEA (dehydroepiandrosterone), SULT1E1/EST (Oestrogen sulfotransferase), STS (Steroid sulfatase), 17β-HSD (17β-Hydroxysteroid dehydrogenase), Oestrone (E1), Oestradiol (E2), Oestrone sulphate (E1-S), Oestradiol sulphate (E2-S).

1.3 Oestrogen Receptors and CRC

Oestrogens exert their effect on cells via ERs, of which there are two forms; ERα discovered in 1966 and located on 6q25 and ERβ found in 1996 and located on 14q23-24.1. Within the colon ERβ is dominant and in CRC an inverse relationship exists between tumour progression and ERβ expression; a reduction in ERβ in CRC is associated with worse stage and grade of disease (21, 22, 23). Hartman et al generated SW480 colon cancer cell lines overexpressing ERβ and found they were mainly in the G1 phase of the cell cycle (24). ERβ knockout mice develop colonic hyperproliferation, loss of differentiation and disordered apoptosis. Also, mice with both APC and ERβ knockouts have larger tumours than APC knockouts alone (23). These findings suggest in normal circumstances ERβ is crucial to colonic cell homeostasis. The underlying mechanism for how ERβ protects against CRC is unknown, but evidence demonstrates that ERβ causes apoptotic effects via DNA fragmentation, increased p53 signalling, up-regulation of caspase 8 and 9 and reduction in β-catenin (24). The presence of ERβ induced apoptosis offers a potential therapeutic intervention, involving ERβ agonists or stimulating overexpression.

1.4 17β-Hydroxysteroid Dehydrogenase

Under normal circumstances there are low levels of aromatase activity in the colon, therefore the predominant metabolite of androstenedione is testosterone, not E1 (Figure 1). This suggests 17β-HSD enzymes are more influential than aromatase. The predominant reaction in normal colonic tissue is oxidative; E2 to E1 via 17β-HSD-2 and this often alters in CRC with loss of 17β-HSD-2 enzyme activity. However, reduced expression of 17β-HSD-2 is associated with an improved outcome (18, 25). Evidence suggests the local rise in E2 concentration inhibits CRC proliferation and induces apoptosis via ERβ (26, 27, 28), or alternatively, high concentrations of E2 may reduce the production of carcinogenic BAs.

Mutations in DNA mismatch repair, also known as colonic microsatellite instability (MSI) is a feature in approximately 15-20% of CRCs and is protected against by E2 (29, 30). Tumours with high 17β-HSD-2 expression and subsequently low E2 concentrations may lack oestrogenic influence offering worse prognosis. Research also suggests that intratumoural E1 can also decrease proliferation in the colon (18). Consequently the protective mechanism of E2, E1 and lowered 17β-HSD-2 against CRC is complex. The biological activity of E1 may be weaker than E2, but it is still a potent oestrogen that can interact with ERβ and be converted to E2 via 17β-HSD-1. Therefore, E1 may be protective by acting as a precursor for E2 and interacting with ERβ.

1.5 STS and EST

Steroid sulphatase (STS) and EST have also shown in human studies prognostic influence on CRC. Sato et al found increased STS/EST expression ratios and resultant local changes in E1 and E2 were associated with a poorer prognosis. Tumours that lacked STS, but expressed EST, had lower intratumoural concentrations of E1 and E2 and an improved outcome (20). This is similar to findings in breast cancer, where STS activity is 50-200 times higher than aromatase activity and expression of STS and EST have an impact on prognosis. This has led to new treatment in breast cancer utilising STS inhibitors (19, 20). Therefore, STS inhibitors may be of benefit to patients with certain types of CRC (20). However, these findings are inconsistent with the 17β-HSD-2 studies, which found that higher concentrations of E1 and E2 improved prognosis. Sato et al did not determine 17β-HSD-2 expression as well as STS/EST status in patient samples. They concluded 17β-HSD-2/17β-HSD-1 expression was unchanged between CRC and normal tissue, as E1 and E2 ratios were similar (20).

Oestrogens clearly have an influential role on CRC development, progression and survival. Evidence conflicts over which enzymes and oestrogens are protective and which are harmful.

Also, risk of CRC differs between endogenous and exogenous oestrogen exposure. There may be subpopulations of CRC that respond differently and perhaps conflictingly. The relationship between CRC and sex hormones needs further characterisation to determine if there is a potential position for manipulation as a treatment for CRC.

2.0 AIMS AND HYPOTHESIS

The aims of this project were to characterise colon cancer cell line oestrogen metabolising capabilities followed by comparison against human tissue samples and related to CRC prognosis. To achieve these aims, methods performed included liquid chromatography/mass spectrometry (LC/MS) to observe the metabolism of E1, E1-S and E2 in various colonic cell lines, FACS analysis to measure the impact of oestrogen on the cell cycle and apoptosis, radiolabelled STS assay, along with Western blot and quantitative PCR for expression of enzymes STS, EST, 17β-HSD-1 and 17β-HSD-2. It is hypothesised that oestrogen will affect CRC patient outcome and can be translated into new therapeutics manipulating local oestrogen concentrations in the colon.

3.0 METHODS

3.1 Cell Culture

Cells were grown in T75 flasks in media supplemented with 10% fetal bovine serum (FBS) and incubated at 37^0C. Colo205 (human Caucasian colon adenocarcinoma) cells were grown in RPMI, WiDR (human colon adenocarcinoma) in MEM, Jeg3 (human choriocarcinoma) in DMEMF12 and HT-29 (human Caucasian colon adenocarcinoma) and HCT116 (human colon carcinoma) in McCoys medium. Once 80% confluent, cells were trypsinised with 0.25% trypsin and split into new flasks. To seed, cells were counted using a haemocytometer and the amount needed for 1 $x10^5$ cells per well in a 6 well plate was calculated. For T25 flasks, cells were seeded at approximately 2.5 x 10^5 cells per flask.

3.2 Human Tissue Samples and Ethics.

Seven female (F) and six male (M) CRC samples were selected based on cancer type (adenocarcinoma) and those with inflammatory bowel disease or known familial mutations were excluded. Females were aged 57-84 and so post-menopausal. Unfortunately, details on their HRT use were not available. Males were aged 53-84 and Duke's staging was: B; F=2, M=2, C; F=4, M=4, D; F=1, M=0 (see appendix 1). CRC tissue, with matched non-cancerous colon tissue, was collected from the Human Biomaterial Resource Centre (HBRC) in accordance with local ethical guidelines. The HBRC is ethically approved by North West 5 Research Ethics Committee, Haydock Park; Ref 09/H1010/75 and authorised to release samples that satisfy their Access Review Panel. All experiments complied with the Human Tissue Act.

3.3 Protein Harvesting

In order to harvest protein from cells the media was removed and the cells washed in phosphate buffered saline (PBS, Sigma). RIPA buffer (Sigma) with protease inhibitor cocktail (Sigma) was added (10µl/1ml of RIPA) as per manufacturer's protocol and incubated at 4^0C for 5 minutes. The plates were scraped and contents collected into Eppendorfs. To clarify, the samples were centrifuged at 8,000g for 10 minutes at 4^0C, the supernatant collected and stored at -20^0C.

To harvest protein from human tissue, 900µl of RIPA buffer and protease inhibitor cocktail was added to approximately 30mg of tissue, before the tissue was lysed with a TissueRuptor device until homogenous (approximately 40 seconds). The homogenate was clarified by centrifugation at 16,000 rpm for 10 minutes at 4^oC and the supernatant collected and stored at -20^0C.

To calculate the amount of protein harvested a Bradford Assay was performed (Sigma) as per manufacturer's instructions.

3.4 RNA Extraction, Reverse Transcription and Real Time PCR

To extract RNA from cell lines and human tissue, Qiagen RNeasy Mini Kit was used as per manufacturer's instructions. The yield and purity of RNA was calculated using 260 absorbance and 260:280 ratio on a nanodrop, conveying RNA in ng/µl.

For the manufacture of cDNA, Tetro cDNA synthesis kit (Bioline) was used as per manufacturer's instructions. The cDNA yield was measured using a picogreen assay (Invitrogen). Real time PCR was performed using TaqMan^{TM} gene expression master mix (Applied Biosystems), coupled with the TaqMan^{TM} gene expression assays (Applied Biosystems) STS, EST, 17β-HSD-2, 17β-HSD-1 and the housekeeping gene RPLPO. 20ng of

cDNA, master mix and probes were loaded onto a 96 well plate, totalling 12µl per reaction and analysed using the program 50^0C 2 minutes, 95^0C 10 minutes, followed by 40 cycles of 95^0C for 15 seconds then 60^0C for 1 minute. The cycle threshold value (Ct) was used for analysis. For STS analysis a standard curve was created using Jeg3 cells. For all other genes of interest ΔCT (gene of interest minus RPLPO) was used to calculate ΔΔCT (ΔCT- ΔCT of control). Control was given the arbitrary number of 1 and samples compared to calculate any fold change ($2^{-\Delta\Delta CT}$). If levels of expression were undetermined, a ΔCt value of 40 was used to allow for numerical analysis.

3.5 Cell Cycle and Apoptosis Using FACS

To determine the effects of oestradiol (E2) on apoptosis and the cell cycle in colon cancer cell lines, Colo205 cells were seeded into T25 flasks as described in section 3.1. Colo205 cells were selected as they had been found to be the most oestrogen responsive. E2 in phenol red free media, along with charcoal stripped FBS (SFBS, Sigma) was applied for 24 or 48 hours at concentrations 0, 1nM, 10nM, 100nM and 1µM. Phenol red free is needed, as phenol can bind to and activate the ER and SFBS contains no oestrogen. This was to ensure that the effects seen on cell cycle and apoptosis were due to the added E2 concentration only. Control wells contained serum complete media with no added E2. The media and trypsinised cells were collected and pelleted. The pellet was re-suspended in phosphate buffered saline (PBS) and divided between two 15ml Falcon tubes, before being centrifuged again and pelleted. Half were re-suspended in 70% ethanol and stored at -20^0C and half were re-suspended in Annexin V binding buffer (Invitrogen). A sample of this was combined with propidium iodide and Annexin V FITC (both Invitrogen) and stored at room temperature in the dark, before being analysed for apoptosis by FACS. When ready for analysis, the cells stored in ethanol were pelleted to remove all ethanol and re-suspended in 2.5µg/ml propidium iodide, then analysed by FACS to determine the effect on the cell cycle.

3.6 STS Assay

3.6.1 Cell Lines

To measure the conversion of estrone sulphate (E1-S) to estrone (E1) by STS in cell lines, the cells were seeded into 6 well plates as described in section 3.1 and incubated at 37^0C in phenol red free media (no FBS) with tritium labelled E1-S for 18 hours. In order to avoid total conversion, unlabelled E1-S was added and to account for procedural losses the cells were also incubated with ^{14}C-E1. The media was collected and E1 and E1-S were separated using toluene extraction. Protein was also harvested as described in section 3.3. The amount of STS activity, converting E1-S to E1, was then counted on a scintillation spectrometer.

3.6.2 Human Tissue Samples

In order to measure the conversion of E1-S to E1 by STS in human samples, tritium labelled E1-S, unlabelled E1-S and ^{14}C-E1 in PBS were added directly to 60µg of protein, harvested as described in section 3.3 and incubated at 37^0C for 4 hours. E1 and E1-S were then separated using toluene extraction and counted on a scintillation spectrometer. To measure the effect of inhibiting STS activity, 0.5µl of 10µM STX64 (Sigma) was added to samples prior to incubation.

3.7 Western Blot

After performing the Bradford Assay, the volume of sample required for 10µg of protein was calculated and added to an equal volume of Laemmli sample buffer (25µl β2-Mercaptoethanol (Aldrich) per 475µl Laemmli Sample Buffer (Bio Rad)) and heated to 95^0C for 5 minutes. Proteins were separated on a 10% SDS-PAGE gel (Protogel, Resolving Buffer, Protogel Stacking Buffer, Protogel (Geneflow), dH_2O, TEMED (Sigma) and 10% Ammonium Persulfate (Sigma)) and then transferred to a PVDF membrane (Immobilon). The

membrane was blocked in 2.5% non-fat milk in TBST (dH_2O, 20g NaCl (Fisher), 0.625ml Tween 80 (Sigma), 50ml 1M Tris (Sigma)). Membranes were than incubated with primary antibody in TBST, washed and then incubated in appropriate HRP conjugated secondary antibody for 1 hour in TBST. Primary antibodies included STS (1:500 with 5% milk, overnight incubation at 4^0C, Abnova), EST (1:400, 2 hour incubation, Abcam), 17β-HSD-1 (1:400, 1 hour incubation, Santa Cruz), and 17β-HSD-2 (1:400 with 1% bovine serum albumin (BSA), overnight incubation, Santa Cruz). ECL western blotting detecting reagent (GE Healthcare) was used as per guidelines and the x-ray film (Kodak) developed on Xograph Compact X4.

3.8 Mass Spectrometry

Cells were seeded into 6 well plates, as described in section 3.1 and incubated at different time points, with differing concentrations of E1, E1-S or E2 in phenol red free media with 10% SFBS. The medium was then collected and stored at -20^0C. In preliminary experiments some cells were lysed with ice cold dH_2O and collected with the medium. After extraction and analysis, as described below, there was no difference in E1, E1-S, E2 or oestradiol sulphate (E2-S) concentrations, with or without cell lysate, so protein was harvested after media collection as described in section 3.3.

In order to establish the concentration of E1, E1-S, E2 and E2-S within the sample media and establish rates of conversion in the cells, an extraction method was developed with the aid of Dr. A. Taylor. For a standard curve, media was spiked with serial concentrations of E1, E2, E1-S and E2-S before extraction. SPE columns (SEP-PAK® Vac 3cc, Waters) were prepared with 2mls 100% methanol and then 2ml water, before media with added internal standard was then passed through the columns. 2mls of methanol was then added and the flow through collected into sylinised glass tubes. This was evaporated at 55^0C with nitrogen flow until dry

before 500µl of 50% methanol/ 50% water was added and then analysed by mass spectrometry. Data was interpreted with the help of Dr A. Taylor.

3.9 Statistical Analysis

Data were compared by student's t-test method to determine statistical significance. Results are expressed as mean ± standard deviation. A p value <0.05 was deemed significant.

4.0 RESULTS

4.1. STS expression varies between colorectal cancer cell lines. Within the oestrogen metabolism pathway (Figure 1) STS enzyme can desulphate E1-S to the more biologically active E1. E1 can then be converted, via 17β-HSD-1, to the most biologically active oestrogen E2. To explore the STS activity in CRC cell lines RNA was reverse transcribed to cDNA and STS expression measured using quantitative PCR. Jeg3 cells, a human choriocarcinoma cell line, are known to have high levels of STS expression and were used as the control. Figure 2 demonstrates the diverseness of STS expression between CRC cell lines. Colo205 cells have the highest STS expression, whereas HCT116, HT-29 and WiDR cells all have low expression. It is worth noting that WiDR cells are derived from HT-29 cells and both are from female CRCs, whereas Colo205 and HCT116 cell lines are derived from male CRCs (31).

Figure 2.

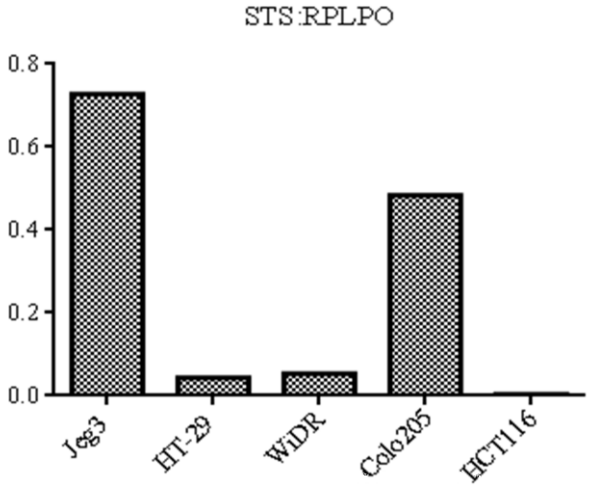

Figure 2. RNA was harvested from CRC cell lines and Jeg3 cells. cDNA was generated from the extracted RNA and real time PCR performed using Taqman^{TM} gene expression assays STS and the housekeeping gene RPLPO. STS:RPLPO ratio expression was compared between CRC cell lines with Jeg3 cells as control. RT-PCR was performed in duplicate.

4.2 STS activity differs between CRC cell lines. As mRNA expression does not always relate directly to levels of enzyme activity, a radiolabelled STS assay was used to measure the

STS activity in CRC cell lines. By adding tritium labelled E1-S to cell media, it was possible to measure the rate of conversion to E1 using a scintillation spectrometer. STX64 is a specific and potent STS inhibitor and as shown in Figure 3, can inhibit the STS activity observed in all cell lines. Comparing Figure 2 and 3, it can be seen that the STS mRNA expression does relate to STS activity in these cell lines. Jeg3 cells have the highest STS expression and Colo205 cells have the greatest activity compared to the other CRC cell lines.

Figure 3.

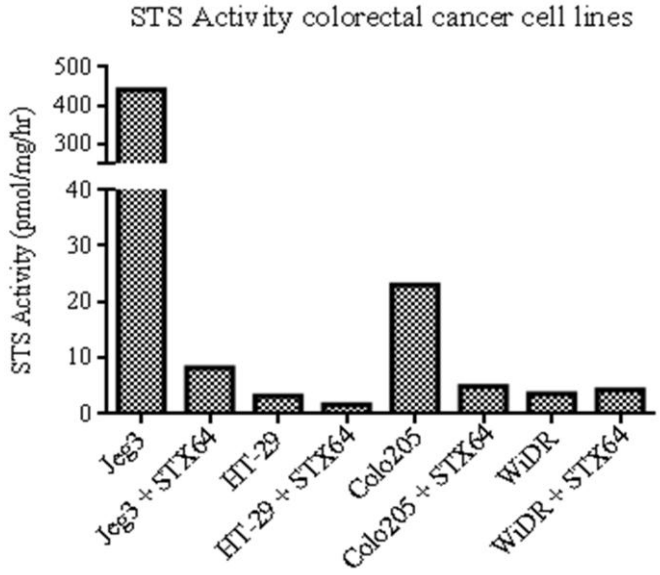

Figure 3. Graph of STS enzyme activity in cell lines, measured in pmol/mg/hr, with Jeg3 cells used as control. STS activity was measured using a radiolabelled STS assay. Cells were exposed to tritium labelled E1-S for 18 hours and conversion to E1 was measured. STX64 is a potent and specific inhibitor of STS and by adding 0.5µl of 10µM STX64 to cells STS activity and so conversion of E1-S to E1 was inhibited. Jeg3 and Colo205 cells can be seen to have high STS activity that can be inhibited by STX64. STS activity experiments were performed in triplicate and STX64 experiments in duplicate.

4.3 Oestradiol has no effect on apoptosis or cell cycle progression. Research by Wilkins et al and Qui et al found that E2 increased apoptosis in Colo205 cells, implying E2 may be detrimental to CRC growth and may explain the reduction in CRC incidence seen with HRT use (27, 28). To replicate these findings Colo205 cells were treated with media containing increasing concentrations of E2. The effect on apoptosis and cell cycle was measured using FACS. Control experiments included complete medium and SFBS medium with no added

E2. After 24 hours (data not shown) there was no change in apoptosis or the cell cycle, so the experiment was extended to 48 hours of treatment. In contrast to published data, Figure 4 demonstrates that 48 hours of treatment with increasing E2 concentrations also had no impact on apoptosis or the cell cycle in Colo205 cells.

Figure 4.

(A)

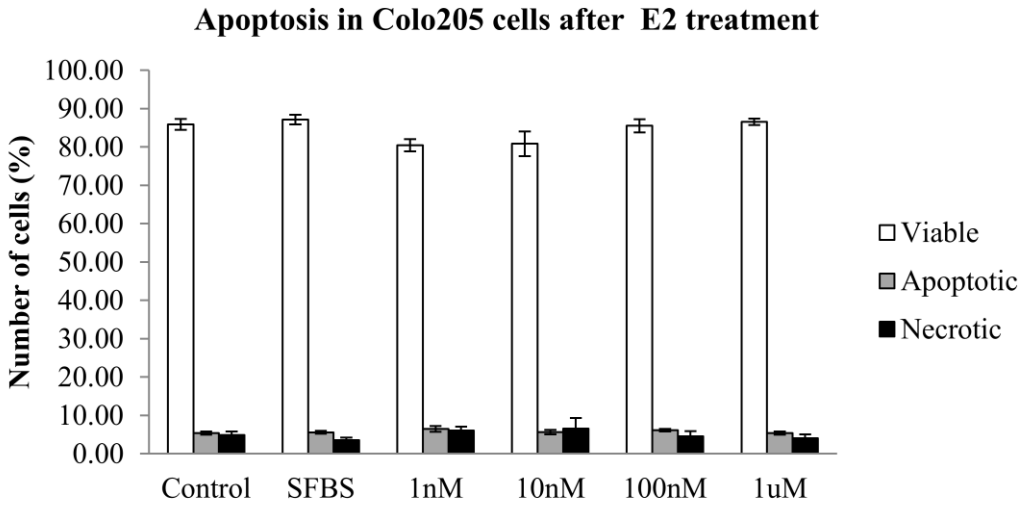

(B)

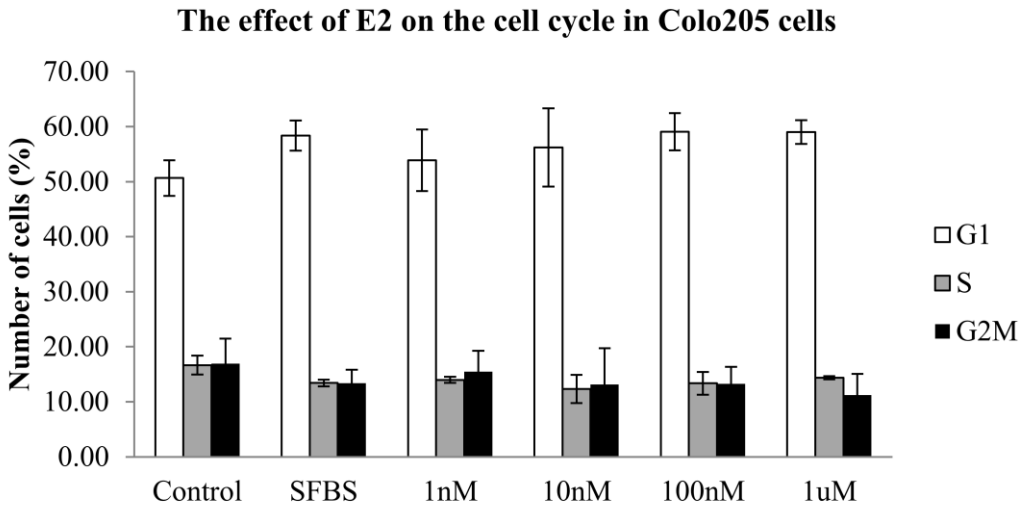

Figure 4. Colo205 cells were treated with E2 at concentrations 0, 1nM, 10nM, 100nM and 1µM for 48 hours. Control samples were cells in complete medium. After E2 treatment the cells were incubated with either (A) Annexin V and propidium iodide before flowcytometry analysis to determine the effect on apoptosis. Or (B) cells were incubated with propidium iodide and analysed by flowcytometry to determine the effect on cell cycle progression. Experiments were done in triplicate.

4.4. Oestrogen metabolism in CRC cell lines. As STS expression and activity was variable between CRC cell lines, it was hypothesised that other oestrogen metabolism pathway enzymes, such as EST and 17β-HSD, would also differ. To investigate, cell lines were treated with medium containing E1, E2 or E1-S. Preliminary experiments optimised treatment length; HCT116 cells were treated for 48 hours and all other cell lines for 1 hour. The activities of STS, EST and 17β-HSD were expected to be reflected by the concentration of oestrogen metabolites within the medium as a result of the treatment. To analyse how cell lines metabolised E1, E2 or E1-S, the cell media after treatment was analysed by LC/MS for oestrogen metabolite concentrations, such as E1, E2, E1-S, E2-S, testosterone and estratriol. Figure 5A, C and E display the overall metabolism of E1-S, E2 and E1 in cell lines respectively. They show that all forms of treated oestrogen were metabolised, but at different rates. Jeg3 and Colo205 cells have high STS activity and so it was expected that E1-S would be metabolised to E1 and E2. However, only Jeg3 cells showed a small increase in E2 (Figure 5B) and there was no increase in E1 (data not shown). Figure 5A also shows that Colo205 cells actually metabolised E1-S much slower that the other cells lines. 17β-HSD-2 oxidises E2 to E1, therefore if cells had 17β-HSD-2 activity, E2 treatment should lead to a rise in E1 concentration; this is shown Figure 5D in HCT116 cells only. In contrast 17β-HSD-1 reduces E1 to E2. As can be seen in Figure 5E, HCT116 cells did not greatly metabolise E1 compared to the other cell lines. Research has found Jeg3 cells highly express 17β-HSD-1 (21) and this is supported by Figure 5F, whereby after E1 treatment Jeg3 media has a rise in E2 concentration. Although there is evidence to partially explain how the oestrogen treatment was metabolised in these cell lines, overall, the majority remains unaccounted for and is presumed to be found in intermediate oestrogen metabolites.

Figure 5.

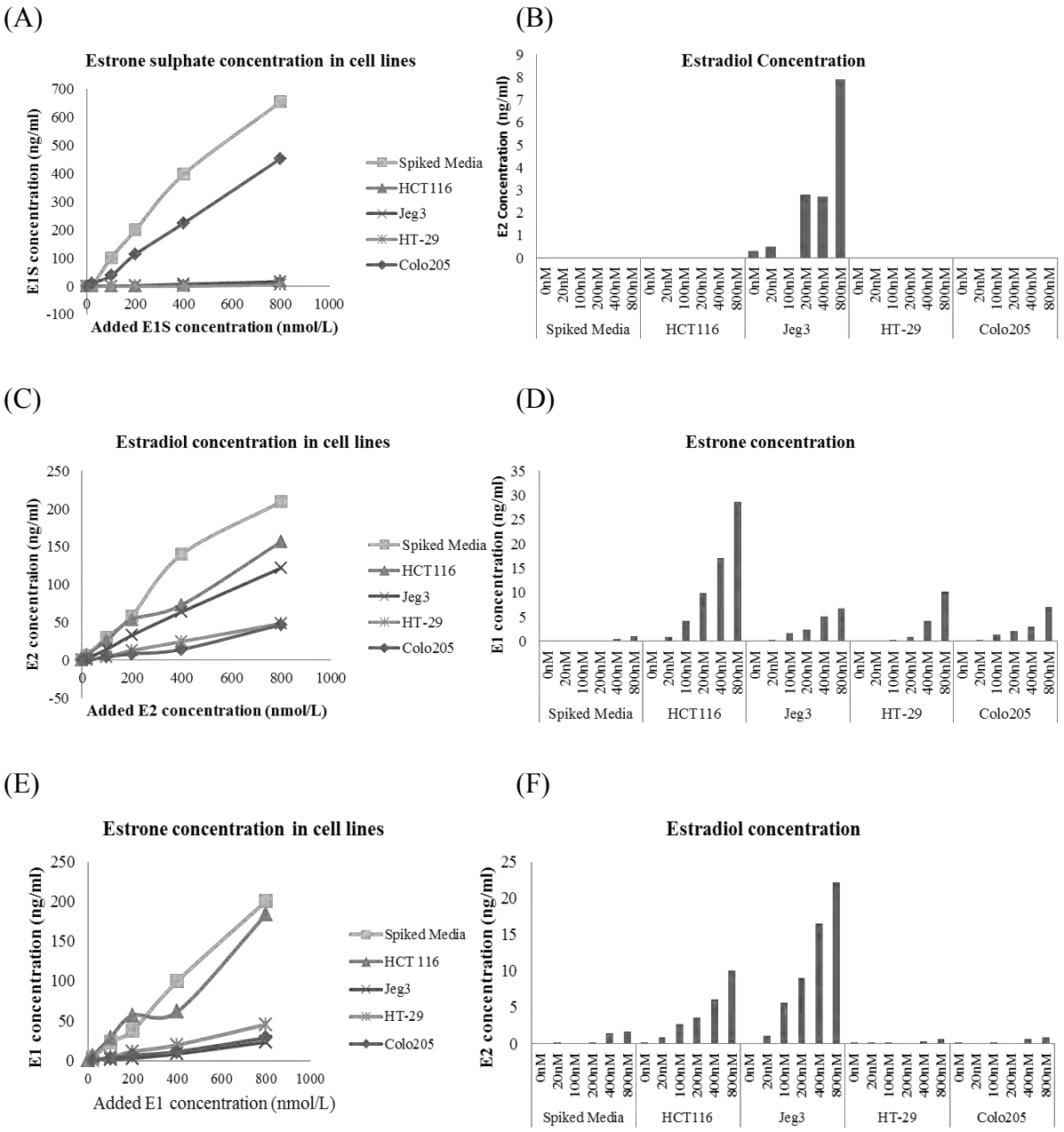

Figure 5. Cells were treated with E1-S, E2 or E1 at concentrations 0, 200nmol, 400nmol, 600nmol and 800nmol. After 48 hours treatment for HCT116 cells and 4 hours for all other cell lines LC/MS analysis of the cell media was performed. LC/MS was used to detect concentrations of oestrogen metabolites within the media before and after treatment (A) Comparison of original E1-S spiked medium with cell line medium concentration of E1-S after treatment. (B) E2 can be seen to increase in Jeg3 cells after E1-S treatment. (C) Summary of E2 spiked medium compared to cell line medium concentrations after treatment. (D) E1 can be seen to increase in HCT116 cells after E2 treatment. (E) Overview of E1 spiked medium and cell line medium concentrations after treatment. (F) E2 can be seen to rise in HCT116 and Jeg3 cell medium after E1 treatment. N=1.

4.5 17β-HSD-2 is reduced in human colorectal cancer tissue. Previous research has shown that 17β-HSD-2, which oxidises E2 to E1, is reduced in CRC tissue when compared to matched normal controls (7, 18). To confirm these findings, seven female CRC tissue samples, with matched normal controls were analysed by RT-PCR for 17β-HSD-2 expression. As can be seen in Figure 6, the female patient's 17β-HSD-2 can be seen to fall in the CRC tissue compared to the non-cancerous tissue (p=0.0001).

Figure 6.

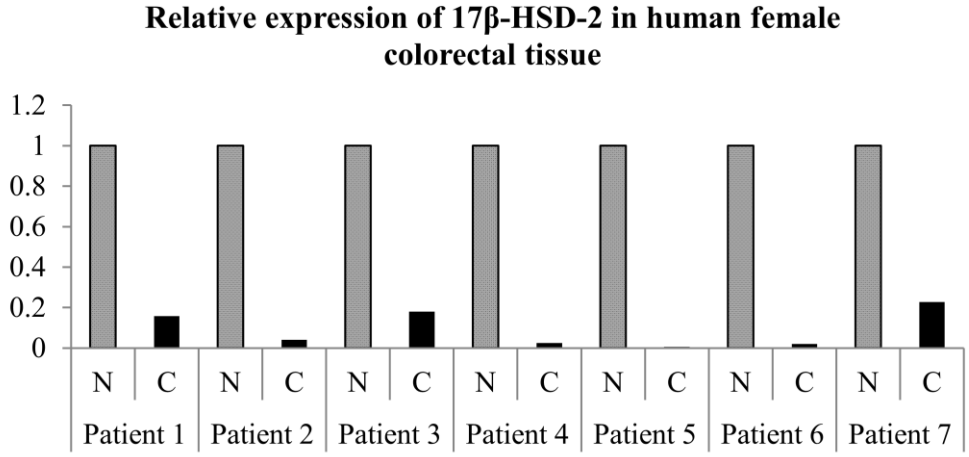

Figure 6. RNA was harvested from female human colorectal tissue. cDNA was generated from extrated RNA and real time PCR perfomred using Taqman^{TM} gene expression assays of 17β-HSD-2 and the house keeping gene RPLPO. 17β-HSD-2 expression in CRC tissue was then compared to matched normal colon tissue. Experiments were permormed in duplicate and statistical significance was determined using student's paired, two-tailed t-test. 17β-HSD-2 expression fell in cancerous tissue compared to matched normal controls, p=0.0001.

4.6. Protein expression differences between normal and cancerous human colorectal tissue. CRC cell lines have differing amounts of oestrogen enzyme expression and activity resulting in variability of oestrogen metabolism. To discover how this compares to human tissue, matched cancerous and normal colorectal tissue from seven females and six males were analysed. Western blots were performed for ERβ, EST, 17β-HSD1, 17β-HSD-2 and STS. Previous research found that ERβ and 17β-HSD-2 were down-regulated in CRC (7, 18, 22). Both female and male Western blots for ERβ were suggestive of reduced ERβ protein in

cancerous tissue (Figure 7A, females patients shown only). Jeg3 cells were used as the control and as previously stated highly express STS. STS protein levels in human samples were low and difficult to detect by Western blot, therefore any alterations between N and C tissue could not be visualised (data not shown). Interestingly EST could only be clearly displayed on the female samples and protein levels showed no clear trend (Figure 7B). EST bands appear at 35kDa and presumed dimer at 70kDa (32, 33). 17β-HSD-1 is increased in some CRC tissue (Figure 7C, males shown only). Unfortunately 17β-HSD-2 could not be clearly seen by Western blot in either males or females (data not shown).

Figure 7.

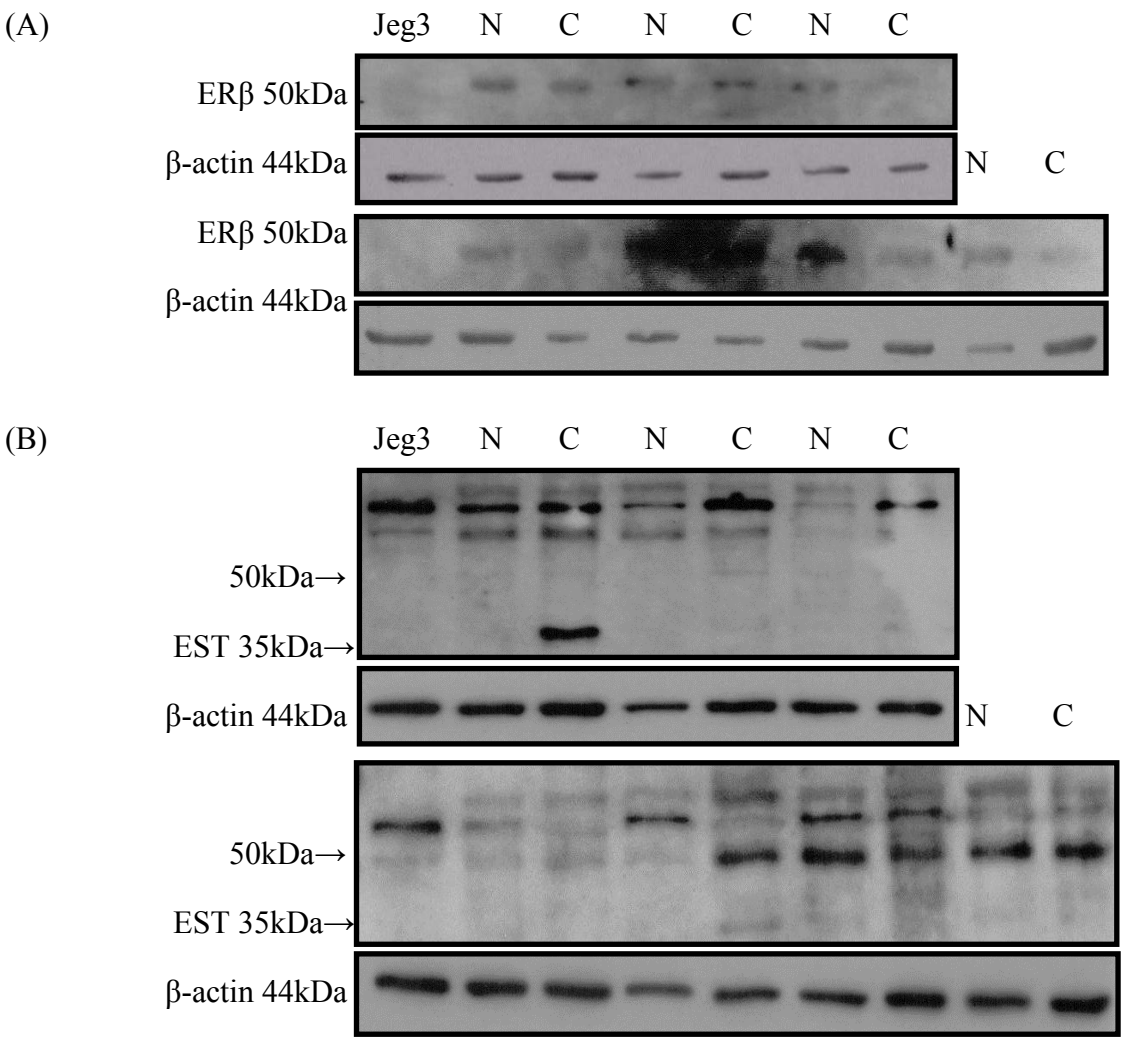

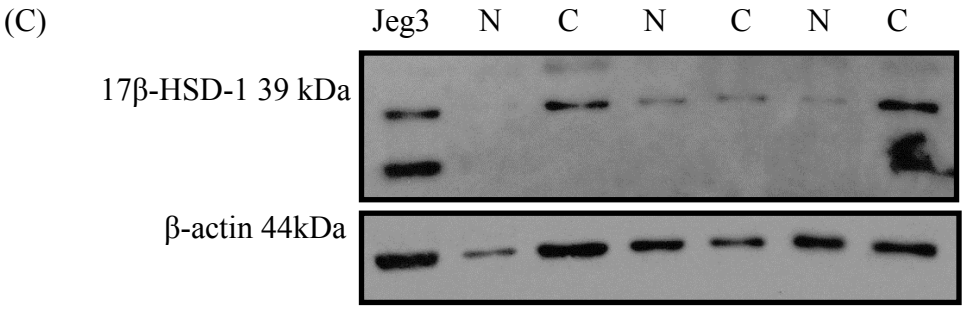

Figure 7. Harvested human tissue protein was separated by SDS-PAGE and subsequent blots probed for ERβ, EST, 17β-HSD-1 and β-actin. Jeg3 cells were used as control and β-actin as loading control. Lanes were laid out as normal (N) followed by matched cancerous (C) colorectal tissue from the same patient and loaded in patient order 1, 2, 3 etc. (A) Western blot image of ERβ in seven female patients. (B) Western blot example of EST in seven female patients. (C) Western blot example of 17β-HSD-1 in three male patients.

4.7 STS activity is increased in human female colorectal cancer. Cell line data demonstrated differences between the CRC cell line, STS expression and activity. It was hypothesised that STS activity would be up-regulated in cancer and drive tumour growth, implying STS inhibitors may be of therapeutic use. To investigate if there was a pattern of STS expression between human normal and CRC tissue, both RNA and protein were extracted from matched normal and cancerous tissue in seven female and six male patients. STS expression was quantified using RT-PCR and activity measured using radiolabelled STS activity assay as described in section 3.6. Figure 8A and B are the results for RT-PCR for male and female patients respectively. In males only there appeared to be a trend of increased STS mRNA in cancerous tissue. However, these results did not correlate with STS activity and overall expression levels of STS were low, making it difficult to calculate noticeable differences between normal and cancerous colorectal tissue. As can be seen in Figure 8C and D, STS activity did show a trend in female, but not male, patients. Only one of the six male patients had a rise in STS activity in the colorectal cancerous tissue (Figure 8C). However, five out of the seven female patients had an increase in STS activity in the cancerous tissue when compared to matched normal controls. This fell slightly short of significance, $p=0.05398$ (Figure 8D). To ensure that STS activity could be inhibited, STX64 was added to

two female patients displaying high STS activity in cancerous tissue. As can be seen in Figure 8E, STX64 was able to inhibit STS activity.

Figure 8.

(A) (B)

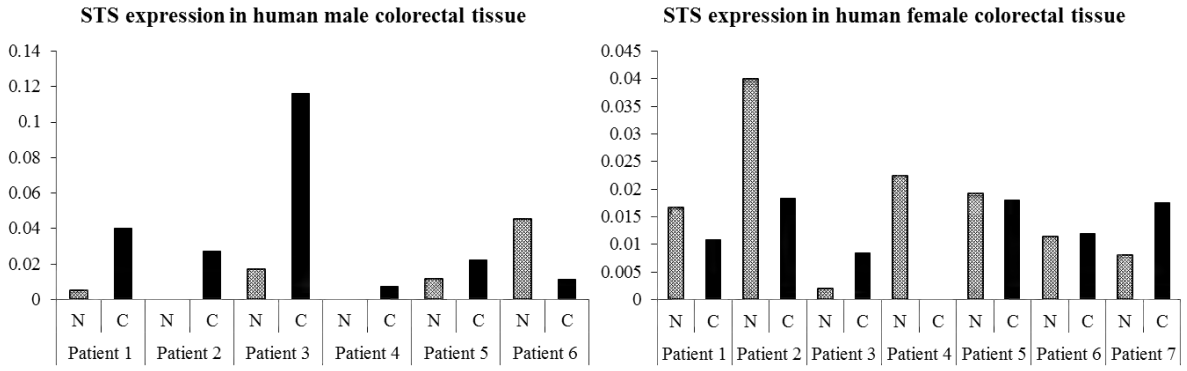

(C) (D)

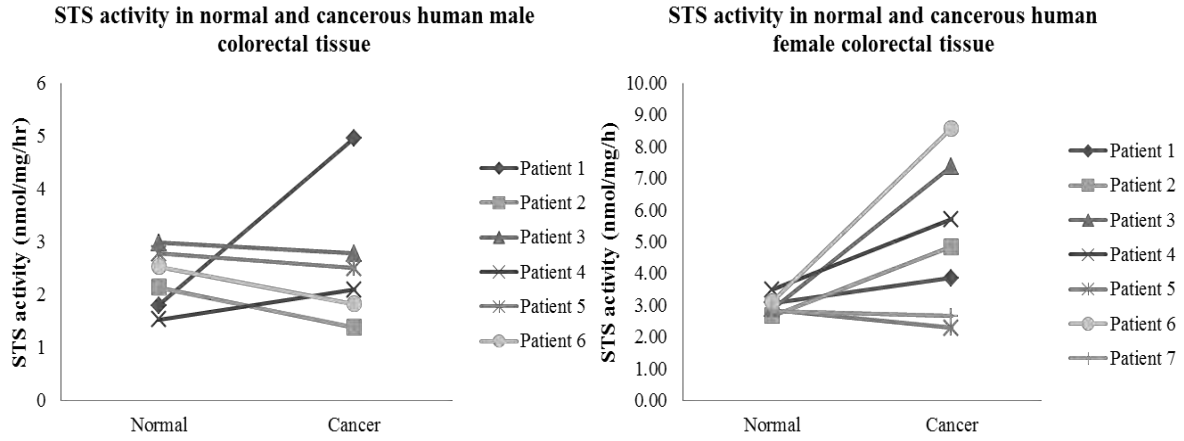

(E)

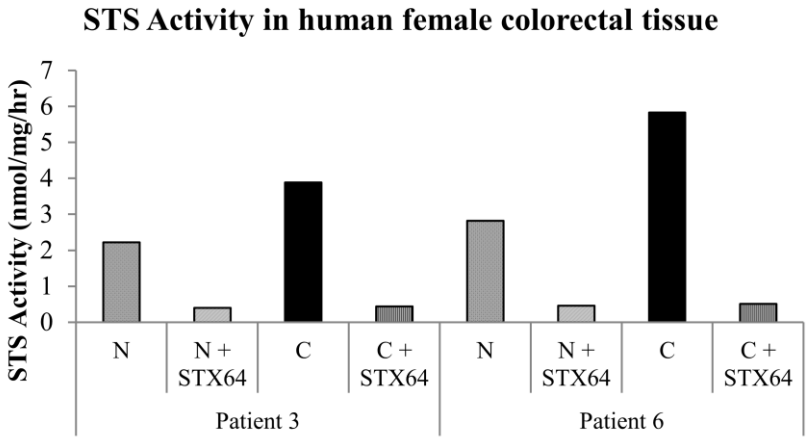

Figure 8. To determine STS enzyme expression cDNA was generated from RNA extracted from human cancerous (C) colorectal tissue and matched normal (N) controls followed by real time PCR using TaqMan^{TM} gene expression assays for STS and the housekeeping gene RPLPO. (A) Normal and cancerous colorectal tissue STS expression in human males. (B) Normal and cancerous colorectal tissue STS expression in human females. STS activity was calculated by adding tritium labelled E1-S to harvested human tissue protein in PBS for 4 hours and measuring the conversion to E1. (C) Comparison of STS enzyme activity between normal and cancerous male colorectal tissue. (D) Comparison of STS enzyme activity between normal and cancerous female colorectal tissue. STX64 is a potent inhibitor of STS. 0.5µl of 10µM STX64 was added to two female patient samples and (E) demonstrates STX64 inhibition of STS activity in these two female patients.

4.0 DISCUSSION

Epidemiological studies and *in vitro* data have suggested a role for oestrogen regulation of colonic epithelial cell growth and development of CRC. Research has demonstrated functional ERs in the gut, with the predominant receptor being ERβ. Therefore ER expression, circulating oestrogen levels, exogenous supply e.g. diet, and local oestrogen synthesis are all possible factors for colorectal carcinogenesis (26). Cell lines and *in vivo* animal model experiments are often used to characterise a cancer, such as CRC, and trial possible therapies prior to human clinical trials. Unfortunately, cell lines are not always truly representative of cancer behaviour and this is reflected by the conflicting findings to date on sex hormones and whether they are protective against or causative of CRC tumourigenesis. In order to uncover differences in CRC cell line behaviour, four were characterised. They included two derived from females (WiDR and HT-29) and two from males (HCT116 and Colo205). This was to investigate if female and male CRC responded similarly to sex hormones. HT-29 and HCT116 cells are both derived from primary colorectal tumours, whereas Colo205 cells originate from ascitic fluid (31). All are known to express ERβ in culture, so are potentially oestrogen responsive (26, 28, 34, 35). As shown in Figure 1, STS is required to convert the biologically inactive E1-S to E1, which can then act on ERs. Previous Western blot data within the lab (unpublished) suggested HCT116 and HT-29 cells had the highest protein levels of STS and Colo205 cells the least. Interestingly RT-PCR data, as shown in Figure 2, displays the opposite findings, with Colo205 cells having the greatest expression levels. Protein levels and mRNA expression do not always reflect enzyme activity. For STS, both post translational alterations and EST expression affecting STS/EST ratio will impact on this. The radiolabelled STS activity assay measures conversion of E1-S to E1, so is a more accurate portrayal of STS activity. This was performed on the cell lines. Despite low protein expression, but in agreement with mRNA expression, Colo205 cells had

the greatest STS activity of the CRC cell lines (Figure 3B). Following the oestrogen metabolism pathway in Figure 1, increased STS activity would lead to higher E1 and potentially E2 concentrations, therefore it is unlikely E1 or E2 would be detrimental to the growth of Colo205 cells. However, as HCT116, HT-29 and WiDr cells had low expression (Figure 2) and HT-29 and WiDr cells low STS activity (Figure 3B), it is hypothesised that E1 or E2 is detrimental to their growth. Supporting this, Weige et al found that E2 did reduce growth in HCT116, LoVo and DLD-1 cells (36). STX64 is a potent STS inhibitor trialled in breast cancer. If STS does enhance CRC tumourigenesis, it may also have a therapeutic role in CRC. Cell lines were treated with STX64 to ensure their STS activity could be inhibited and as can be seen in Figure 3, STX64 reduced STS activity in cell lines.

Controversy exists as to whether oestrogen is protective or involved in CRC tumourigenesis. If E1 or E2 were detrimental to cell survival, it may be predicted that it would be metabolised to a less biologically active oestrogen such as E1-S, increase apoptosis and halt progression through the cell cycle. If E1 or E2 actually enhances tumour growth, there may be reduced apoptosis and enhanced cell division. Research by Weige et al demonstrated that E2, when applied to non-malignant colonocytes, was protective against tumour development by increasing apoptosis. However, when given to CRC tissue, this effect was lost (36). This is supportive of the WHI trial for HRT use. Exogenous HRT was found to reduce CRC incidence. However, women diagnosed with CRC, whilst taking HRT, were found with more advanced disease (17). In contrast to these findings studies, such as those by Wilkins et al (27) and Qui et al (28), have demonstrated that oestrogens have a protective effect on the colon by increasing apoptosis in CRC cell lines, such as Colo205 cells after E2 treatment. As already stated, Colo205 cells were found to have increased STS activity compared to other cell lines (Figure 3B), increasing E1 and possibly E2 concentrations. It seems unlikely this would occur if E1 or E2 were detrimental to their growth.

To investigate this discrepancy Colo205 cells were treated with medium containing increasing E2 concentrations for 24 and 48 hours. Using FACS analysis, apoptosis and changes in cell cycle were measured. Supporting STS activity findings in Figure 3B, even at concentrations of 1μM for 48 hours, E2 had no impact on apoptosis or cell cycle (Figure 4). It would be beneficial to repeat this experiment on CRC cell lines with lower STS activity, such as HT-29 cells, as it may offer insight into the way the different cell lines react.

In order to observe how oestrogen is metabolised in CRC cell lines, they were treated with medium containing E1-S, E2 or E1. The medium was later collected and analysed by LC/MS for oestrogen and its metabolites. Figure 5A, C and E are overviews of E1-S, E2 and E1 metabolism by the cell lines respectively. As can be seen in these three graphs, Colo205 and HT-29 cells rapidly (within 1 hour) metabolised E1-S, E2 and E1 from their media; what the oestrogen was metabolised to is unknown (Figure 5B, D and F) and HCT116 cells metabolised the oestrogen more slowly (over 48 hours). In Figure 5C it can be seen that HCT116 cells oxidised some E2 to E1 and in Figure 5F a small amount of E1 was reduced to E2, but the majority was unaccounted for. If oestrogen was detrimental to cell growth it could be expected to be metabolised to a less biologically active metabolite over time. However, E1-S did not rise after E1 treatment (data not shown) and E1-S was also metabolised away (Figure 5A). Another possibility is the applied oestrogen was converted to a more growth enhancing metabolite that has not yet been identified. For these reasons, it would be interesting to re-examine the medium for 16α-hydroxyestrone, 2-hydroxyestrone, 2-methoxyoestrone and 2-methoxyestradiol. 16α-hydroxyestrone is biologically active, however, the extent of biological activity of 2-hydroxyestrone is controversial. Evidence is accumulating that the ratios of these two metabolites are important in breast cancer outcome (37). Research is also suggestive that 2-methoxyestrone and 2-methoxyestradiol can inhibit

angiogenesis (38) and 2-methoxyestradiol is undergoing clinical trials in metastatic carcinoid tumours (39). Figure 9 demonstrates where these metabolites fit into the oestrogen pathway.

Figure 9.

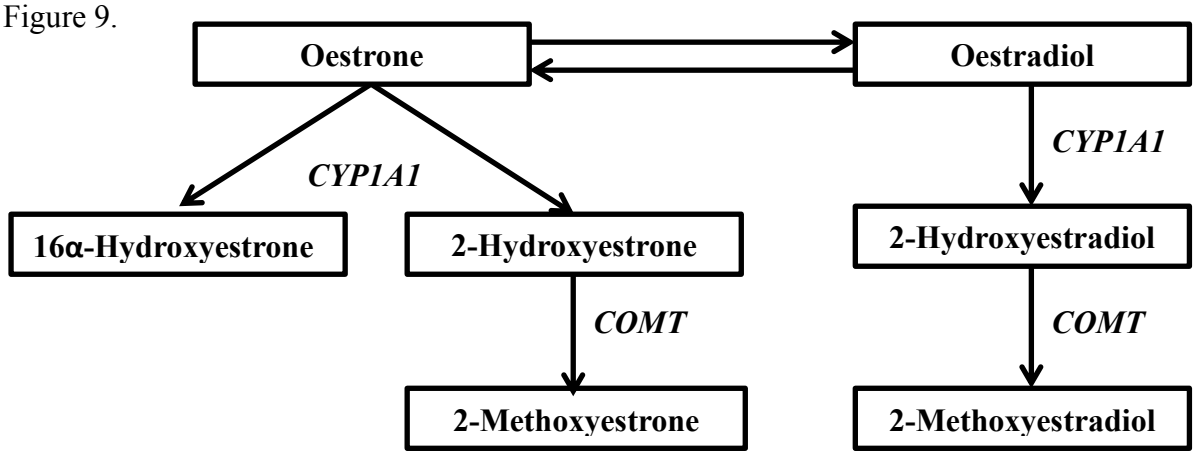

Figure 9. Flow diagram of extended oestrogen metabolism pathway. CYP (Cytochrome P450), COMT (catechol-O-methyltransferase).

Previous research has shown 17β-HSD-2 is often down-regulated in cancer (18, 25), suggesting a local rise in E2 and reduction in E1 concentrations. Down-regulation of 17β-HSD-2 in CRC has also been associated with improved survival. Theories surrounding this suggest that the alteration in E2 and E1 is protective against tumourigenesis and CRC, that is more oestrogen responsive, has a better outcome. To further examine these findings RNA was extracted from human tissue samples and 17β-HSD-2 expression measured by RT-PCR. Only female data were available, but was supportive of these studies, showing a reduction in 17β-HSD-2 in all seven patients (Figure 6, $p=0.0001$).

Supporting current literature, Figure 7A demonstrates female patients' ERβ protein expression; ERβ levels appear lower in the cancerous tissue compared to matched normal controls (21, 22, 23). Unfortunately, EST protein expression was only available for the female patients. It is possible that male expression is low, therefore was not detected by the Western blot antibody. There was no clear trend for EST protein in the females (Figure 7B) and EST appeared more clearly as a dimer (32, 33). For patients 1-3 and 5, EST increased in

cancerous tissue, but in patients 4, 6 and 7 levels are similar in normal and cancerous tissue. The male patients had the clearest 17β-HSD-1 blots. They show that 17β-HSD-1 protein levels are higher in cancerous tissue when compared with matched normal controls (Figure 7C). Other studies have found mixed results. For example, Rawluszko et al found reduced 17β-HSD-1 in cancer of the proximal colon, but not in distal or rectal cancers (40). However, if E2 was promoting tumour growth, a down-regulation of 17β-HSD-2 expression and rise in17β-HSD1 would lead to an increase in E2 concentration, especially when coupled with an increase in STS expression. Unfortunately, 17β-HSD-2 RT-PCR data is not yet available for the male patients and Western blots for STS revealed low levels that could not be compared (data not shown). The Western blot data (Figure 7) did not give a clear picture as to changes that occur in the colon during carcinogenesis.

STS activity assays were performed on all human tissue samples in addition to RT-PCR. mRNA expression levels of STS were low, as suspected from Western blot attempts (Figure 8A and B). This created difficultly accurately calculating differences in STS expression between samples. In male samples there appeared a trend; STS mRNA expression was increased in cancer. However, as stated, STS expression was low overall, therefore RT-PCR needs to be repeated with a greater amount of cDNA to amplify any differences, if any, between normal and cancerous colorectal tissue. The STS activity data did show a trend between normal and malignant colorectal tissue and between male and female patients. In contrast to RT-PCR data, five out of the six male patients had no change in STS activity between cancerous and matched normal colorectal tissue (Figure 8C). However, five out of the seven female patients had an increase in STS activity in cancerous tissue (Figure 8D). This trend fell short of significance ($p=0.05398$). Figure 8E demonstrates the rise in STS activity in female patients was able to be inhibited by STX64. In female patients, the rise in STS activity and fall in 17β-HSD-2 expression supports the notion that E2 drives

tumourigenesis in the colon. The Colo205 data, which demonstrated a rise in STS activity and E2 that did not lead to apoptosis, contributes to existing evidence that oestrogen aids tumour growth. The difference between male and female STS activity was unexpected. However, when it is considered that the majority of cancers occur from polyps and accumulate mutations over 5-10 years before becoming malignant, it is possible that female CRCs may begin in a more oestrogenic environment, altering their growth behaviour compared to male CRC. Unfortunately, there was no follow-up information from the samples used, with which to determine whether the differences seen between males and females and those samples with raised STS activity, affected patient outcome. Sato et al measured STS/EST ratio and total intratumoural oestrogen concentrations, comparing cancerous colorectal tissue to matched normal tissue. They found high intratumoural oestrogen was associated with a worse outcome and -/+ group of STS/EST status was inversely associated with Dukes' stage and depth of invasion; lower STS was associated with improved outcome (20).

The aim of this project was to characterise CRC cell line oestrogenic profiles and relate oestrogen metabolism to prognosis in human samples. Unfortunately, follow-up on the patients was not available therefore results could not be related to prognosis. Future work includes completion of cell line characterisation with RT-PCR for EST, establishing 17β-HSD-1 and 17β-HSD-2 mRNA expression in human CRC, development of an EST activity assay, in addition to expanding the number of human samples. Also, the impact of STS inhibition or STS knockdown in CRC cell lines and the effect on growth and invasion.

Findings from this project suggest E1 and E2 drive CRC tumourigenesis when associated with raised STS activity. Therefore, as with breast cancer, STS inhibitors could be a life-prolonging therapy in CRC. Cancer does not respond identically in patients and emerging

evidence suggests subpopulations of CRC exist. Some CRCs are oestrogen responsive and as we enter the era of personalised medicine it is this branch of patients that will benefit most from endocrine therapy.

APPENDIX 1

(i) Table 2

ANATOMICAL SITE OF TISSUE	HBRC No	SPECIMEN TYPE	PATIENT'S AGE AND SEX	PATHOLOGICAL DIAGNOSIS	TNM STAGING	DUKE'S CLASSIFICATION
Anterior resection for recto-sigmoid	13654	Normal sigmoid Colon	81 F	Adenocarcinoma distal sigmoid colon	pT3 N1 Mx	C1
	13655	Normal sigmoid Colon				
	13656	Tumour sigmoid colon				
	13657	Tumour sigmoid colon				
Sigmoid colon	13658	Tumour sigmoid colon	73F	Adenocarcinoma sigmoid colon (Foxtrot trial)	YpT3 No Mx	B
	13659	Tumour sigmoid colon				
	13660	Normal sigmoid Colon				
	13661	Normal sigmoid Colon				
Right colon	13662	Caecal tumour	57F	MSI-H adenocarcinoma with loss of MLH1 and PMS2 expresion and BRAF mutation within codon 600	pT2 N1	C
	13663	Normal colon				
	13664	Normal colon				
	13665	Caecal tumour				
Colon	13666	Normal bowel	84F	Adenocarcinoma, caecum	pT4 N0 Mx	
	13667	Tumour bowel				
Right colon	13668	Normal colon	72F	Caecum: MSI high adenocarcinoma	pT3 N2	C
	13669	Colorectal cancer				
Sigmoid colon	13670	Normal colon	71F	Invasive sigmoid colon adenocarcinoma	pT4 (4b-TNM 2005) N1 Mx	C1
	13671	Sigmoid cancer				
Anterior resection rectum	13672	Normal colon	68F	Adenocarcinoma, sigmoid/upper rectum	pT3 N1 M1(liver and lung metastases).	
	13673	Rectosigmoid tumour				

Table containing details of the female human tissue samples used

(ii) Table 3

ANATOMICAL SITE OF TISSUE	HBRC No	SPECIMEN TYPE	PATIENT'S AGE AND SEX	PATHOLOGICAL DIAGNOSIS	TNM STAGING	DUKE'S CLASSIFICATION
Right colon	14780	Normal Colon	76M	Advance caecal adenocarcinoma	pT4 N2	C
	14781	Normal Colon				
	14782	Tumour colon				
	14783	Tumour colon				
Colorectal sigmoid, Hartman's procedure	14784	Normal colon	75M	Adenocarcinoma upper rectum	YpT3 N1 Mx	
	14785	Colorectal cancer				
Segment of bowel	14786	Normal colon	55M	Left colon adenocarcinoma	pT4 N0	B
	14787	Colorectal cancer				
Sigmoid colon	14788	Normal sigmoid colon	75M	Invasive sigmoid colon adenocarcinoma	pT3 N0 Mx	B
	14789	Normal sigmoid colon				
	14791	Tumour colon				
Total colectomy (open)	14792	Normal colon	53M	Invasive adenocarcinoma of splenic flexure and sigmoid colon. Tumours invade serosa,extramural lymphovascular invasion	pT4 (both tumour) N2 Mx	C1
	14793	Sigmoid tumour				
	14794	Splenic tumour				
Sigmoid colon	14795	Tumour colon	84M	Adenocarcinoma	pT4 N2	C
	14796	Normal colon				
Right hemicolectomy	14797	Normal colon	64M	Adenocarcinoma, well to moderately differenciated, with extracellular mucin production	pT3 N0 Mx	B
	14798	Tumour colon				

Table containing details of the male human tissue samples used

REFERENCES

1. Cancer Research UK (2012). CancerStats report- Colorectal Cancer. Cancer Research UK (23/07/2012) http://publications.cancerresearchuk.org/downloads/Product/CS_KF_BOWEL.pdf
2. Degirolamo C, Modica S, Palasciano G, Moschetta A. Bile acids and colon cancer: Solving the puzzle with nuclear receptors. *Trends Mol Med*. 2011; 17 (10): 564-572
3. McCracken M, Olsen M, Chen MS, Jemal A, Thun M et al. Cancer Incidence, Mortality and Associated Risk Factors Among Asian Americans of Chinese, Filipino, Vietnamese, Korean and Japanese Ethnicities. *CA Cancer J Clin*. 2007; 57: 190-205
4. Dukes CE, Bussey HJ. The Spread of Rectal Cancer and its Effect on Prognosis. *Br J Cancer*. 1932; 12: 309-320
5. John Hopkins Colon Cancer Centre (2012). Staging of Colorectal Cancer (23/07/2012). http://www.hopkinscoloncancercenter.org/CMS/CMS_Page.aspx?CurrentUDV=59&CMS_Page_ID=EEA2CD91-3276-4123-BEEB-BAF1984D20C7
6. Cancer Research UK (2012). Types of Treatment for Bowel Cancer. Cancer Research UK (23/07/2012). http://cancerhelp.cancerresearchuk.org/type/bowel-cancer/treatment/which-treatment-for-bowel-cancer
7. English MA, Stewart PM, Hewison M. Estrogen metabolism and malignancy: analysis of the expression and function of 17β-hydroxysteroid dehydrogenases in colonic cancer. *Mol Cell Endocrinol*. 2001; 171: 53-60
8. Wynder EL, Shigematsu T. Environmental Factors of Cancer of Colon and Rectum. *Cancer*. 1967; 20(9): 1520-1561
9. De Jong UW, Day NE, Muir CS, Barclay THC, Bras G et al. The distribution of cancer within the large bowel. *Int J Cancer*. 1972; 10(3): 463-477
10. Narayan S, Rajakumar G, Prouix H, Singh P. Estradiol is trophic for colon cancer in mice: effect on ornithine decarboxylase and c-myc messenger RNA. *Gastroenterology*. 1992; 103(6): 1823
11. Garland P, Rodesch F, Leroy F, Chretien J. Altered Duration of DNA Synthesis and Cell Cycle in Non-targeted Tissues of Mice treated with Oestrogen. *Nature*. 1967; 216: 1211-1212
12. Hoff MB, Chang WWl, Mak KM. The effect of oestrogen on cell proliferation in colonic mucosa of the mouse. *Virchows Arch B Cell Path Inc Mol Path*. 1981; 35(1): 263-273
13. Fraumeni JF Jr, Lloyd JW, Smith EM, Wagoner JK. Cancer mortality among nuns: role of marital status in aetiology of neoplastic disease in women. *JNCI*. 1969; 42: 455-68.
14. McMichael AJ, Potter JD. Reproduction, endogenous and exogenous sex steroids, and colon cancer: a review and hypothesis. *JNCI*. 1980; 65: 1201-1207.
15. Zervoudakis A, Strickler HD, Park Y, Xue X, Hollenbeck A, Schatzkin A, Gunter MJ. Reproductive history and risk of colorectal cancer in postmenopausal women. *JNCI*. 2011; 103(10): 826-34.

16. Rose DP, Boyar AP, Wynder EL. International comparisons of mortality rates for cancer of the breast, ovary, prostate, and colon, and per capita food consumption. *Cancer*. 1986; 58(11): 2363-2371
17. Rossouw JE, Anderson GL, Prentice RL, LaCroix AZ, Kooperberg C. et al. Risks and Benefits of estrogen Plus progestin in Healthy Postmenopausal Women: Principal Results From the Women's health Initiative randomized Controlled Trial. *JAMA*. 2002; 288(3): 321-333.
18. English MA, Hughes SV, Kane KF, Langman MJS, Stewart PM et al. Oestrogen inactivation in the colon: analysis of the expression and regulation of 17β-hydroxysteroid dehydrogenase isozymes in normal and colonic cancer. *Br J Cancer*. 2000; 83 (4): 550-558
19. Chetrite GS, Cortes-Prieto JC, Philippe JC, Wright F, Pasqualini JR. Comparison of oestrogen concentrations, estrone sulfatase and aromatase activities in normal, and in cancerous, human breast tissues. *J Steroid Biochem Mol Biol*. 2000; 72: 23-27
20. Sato R, Suzuki T, Katayose Y, Miura K, Shiiba K et al. Steroid Sulfatase and Estrogen Sulfotransferase in Colon Carcinoma: Regulators of Intratumoral Estrogen Concentrations and Potent Prognostic Factors. *Cancer Res*. 2009: 69: 914-922
21. Zhang CY, Chen J, Yin DC, Lin SX. The Contribution of 17beta-Hydroxysteroid Dehydrogenase Type 1 to Estradiol-Estrone Ratio in estrogen-Sensitive Breast Cancer Cells. *Plos One*. 2012; 7
22. Kuiper GGJM, Shughrue PJ, Merchenthaler I, Gustafsson JÅ. The Estrogen Receptor β Subtype: A Novel Mediator of Estrogen Action in Neuroendocrine Systems. *Front Neuroendocrinol*. 1998; 19: 253-286
23. Kennelly R, Kavanagh DO, Hogan AM, Winter DC. Oestrogen and the colon: potential mechanisms for cancer prevention. *Lancet Oncol*. 2008; 9: 385-391
24. Hartman J, Edvardsso K, Lindberg K, Zhao C, Williams C et al. Tumor Repressive Function of Estrogen Receptor β in SW480 Colon Cancer Cells. *Cancer Res*. 2009; 69: 6100-6106
25. English MA, Kane KF, Cruickshank N, Langman MJ, Stewart PM, Hewison M. Loss of estrogen inactivation in colonic cancer. *J Clin Endocrinol Metabol*. 1999; 84: 2080-2085.
26. Fiorelli G, Picariello L, Martineti V, Tonelli F, Brandi ML. Estrogen synthesis in human colon cancer epithelial cells. *J Steroid Biochem Mol Bio*. 1999; **71:** 223–230
27. Wilkins HR, Doucet K, Duke V, Morra A, Johnson N. Estrogen prevents sustained COLO-205 human colon cancer cell growth by inducing apoptosis, decreasing c-myb protein, and decreasing transcription of the anti-apoptotic protein bcl-2. *Tumour Biol*. 2010; 31(1): 16-22
28. Qiu Y, Waters CE, Lewis AE, Langman MJS, Eggo MC. Oestrogen-induced apoptosis in colonocytes expression oestrogen receptor β. *J Endocrinol*. 2002; 174(3): 369-377
29. Jensen SA, Vainer B, Kruhøffer, Sørensen J. Microsatellite instability in colorectal cancer and association with thymidylate synthase and dihydropyrimidine dehydrogenase expression. *BMC Cancer*. 2009; 9(25)

30. Slattery ML, Potter JD, Curtin K, Edwards S, Ma KN et al. Estrogens Reduce and Withdrawal of Estrogens Increase Risk of Microsatellite Instability-positive Colon Cancer. *Cancer Res*. 2001; 61: 126-130
31. ATCC (2012). (24/07/2012). www.atcc.org
32. Stjernschantz E, Reinen J, Meinl W, George BJ, Glatt H et al. Comparison of murine and human estrogens sulfotransferases inhibition *in vitro* and *in silico*- Implications for differences in activity, subunit dimerization and substrate inhibition. *Mol Cell Endocrinol*. 2010; 317: 127-140
33. Petrotchenko EV, Pedersen LC, Borchers CH, Tomer KB, Negishi M. The dimerization motif of cytosolic sulfotransferases. *FEBS Letters*. 2001; 490: 39-43
34. Hogan AM, Collins D, Baird AW, Winter DC. Estrogen and gastrointestinal malignancy. *Mol Cell Endocrinol*. 2009; 307: 19-24
35. Fiorelli G, Picariello L, Martineti V, Tonelli F, Brandi ML. Functional Estrogen Receptor β in Colon Cancer Cells. *Biochem Biophys Res Commun*. 1999; 261: 521-527
36. Weige CC, Allred KF, Allred CD. Estradiol Alters Cell Growth in Nonmalignant Colonocytes and Reduces the Formation of Preneoplastic Lesions in the Colon. *Cancer Res*. 2009; 69: 9118-9124
37. Ursin G, London S, Stanczyk FZ, Gentzschein E, Paganini-Hill A et al. Urinary 2-Hydroxyestrone/16α-Hydroxyestrone ratio and Risk of Breast Cancer in postmenopausal Women. *JNCI*. 1999; 91(12): 1067-1072
38. Newman SP, Leese MP, Purohit A, James DRC, Rennie CE et al. Inhibition of *in vitro* angiogenesis by 2-methoxy- and 2-ethyl-estrogen sulfamates. *Int J Cancer*. 2004; 109: 533-540
39. Kulke MH, Chan JA, Meyerhardt JA, Zhu AX, Abrams TA et al. A prospective phase study of 2-methoxyestradiol administration in combination with bevacizumab in patients with metastatic carcinoid tumours. *Cancer Chemother Pharmacol*. 2011; 68(2): 293-300
40. Rawluszko AA, Horbacka K, Krokowicz P, Jagodziński PP. Decreased expression of 17β-hydroxysteroid dehydrogenase type 1 is associated with DNA hypermethylation in colorectal cancer located in the proximal colon. *BMC Cancer*. 2011; 11: 522